Journal of Medicinal Chemistry

Article

Cite This: J. Med. Chem. XXXX, XXX, XXX−XXX

pubs.acs.org/jmc

Development of Peptide-Based Sirtuin Defatty-Acylase Inhibitors Identified by the Fluorescence Probe, SFP3, That Can Efficiently Measure Defatty-Acylase Activity of Sirtuin

Mitsuyasu Kawaguchi, Naoya Ieda, and Hidehiko Nakagawa*

Graduate School of Pharmaceutical Sciences, Nagoya City University, 3-1 Tanabe-dori, Mizuho-ku, Nagoya, Aichi 467-8603, Japan

Supporting Information

ABSTRACT: Sirtuins (SIRTs) are a family of nicotinamide adenine dinucleotide-dependent histone deacetylases that serve as epigenetic regulators of many physiological processes. Recent studies have shown that in addition to their well-known deacetylase activity, sirtuins also exhibit deacylase activity, such as demyristoylase activity. Here, we show that our previously reported sirtuin fluorescence probe, SFP3, can measure the defatty-acylase activity of SIRT1−3, enabling selective assay of the deacylase activity. We further utilized this finding to develop the first inhibitors of SIRT2 defatty-acylase activity. Notably, most previously reported sirtuin inhibitors, including compound **TM**, AGK2, and SirReal2, showed almost no SIRT2 defatty-acylase-inhibitory activity, but are essentially specific deacetylase inhibitors. These results suggest that the active sites catalyzing the deacetylase and defatty-acylase activities of sirtuins may be independent.

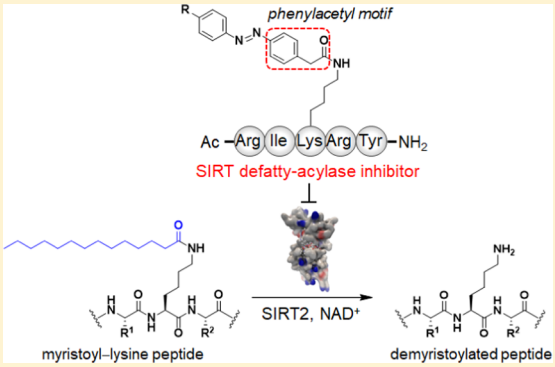

INTRODUCTION

Human sirtuins (SIRT1−7) are a family of nicotinamide adenine dinucleotide (NAD^+)-dependent histone deacetylases that function as epigenetic regulators, and their activities are correlated with cellular energy levels, that is, the NAD^+−NADH ratio regulates their activities.[1,2] Their catalytic activities toward histone proteins and nonhistone proteins, including transcription factors and metabolic enzymes, play important roles in many physiological and pathological functions, including metabolic regulation, stabilization of genomic DNA, stress responses, and cancers.[3−6]

For a long time, it was thought that sirtuins only catalyze deacetylation reactions of histones and the adenine diphosphate-ribosylation reaction. However, more recently, it was found that some sirtuins (SIRT4−7) exhibit quite weak deacetylase activity but have relatively strong deacylase activities instead; for example, SIRT4 shows lipoamidase activity, SIRT5 shows desuccinylase and demalonylase activities, SIRT6 shows demyristoylase activity, and SIRT7 shows desuccinylase activity.[7−10] In addition, SIRT1−3, which has strong deacetylase activity, can also efficiently remove long-chain fatty acid-derived acyl groups at the ε-amino group of lysine residues, that is, they have defatty-acylase activity.[11] These intriguing findings were supported by X-ray crystallographic data showing the existence of a large hydrophobic pocket in SIRT2 and SIRT6 that can accommodate the myristoyl group.[12,13]

Protein fatty acylation is important for anchoring proteins to the cell membrane and plays significant roles in cell signaling and protein−protein interactions.[14] Early studies focused on N-terminal glycine myristoylation and cysteine palmitoylation, but little is known about the biological significance of lysine fatty acylation.[15] Recent reports suggest that SIRT6 demyristoylase activity regulates the secretion of TNF-α[9] and that SIRT2 defatty-acylase activity regulates the localization of K-Ras4a oncoprotein and promotes cellular transformation.[16] Interestingly, a study of the SIRT6 G60A mutant, which possesses defatty-acylase activity but lacks deacetylase activity, demonstrated that the deacetylase and defatty-acylase activities of SIRT6 regulate independent cellular functions, for example, having roles in transcriptional regulation and protein secretion, respectively.[17]

Many SIRT2 "deacetylase" inhibitors have been reported,[18−22] but their "defatty-acylase"-inhibitory activities have hardly been examined.[23−27] This is an important lacuna because specific defatty-acylase inhibitors would be useful not only for basic biological studies but also as candidate therapeutic agents, for example, for inflammation and cancer.

Therefore, in this study, we set out first to establish an assay system for measuring SIRT defatty-acylase activity and, second, to use the developed assay to discover SIRT2 defatty-acylase inhibitors based on the structure of the SIRT2 inhibitor **RIK^{Tfa}RY** reported by Suga and co-workers.[28] To evaluate SIRT2 defatty-acylase activity, we used two indicators, that is, our recently reported sirtuin fluorescence probe, SFP3,[29] and a fluorescence probe, **p53(Myr)-AMC**, developed to monitor demyristoylase activity. A study of a series of newly synthesized

Received: February 18, 2019
Published: May 22, 2019

DOI: 10.1021/acs.jmedchem.9b00315
J. Med. Chem. XXXX, XXX, XXX−XXX

Chart 1. Structures of Dabcyl Derivatives Used in This Study

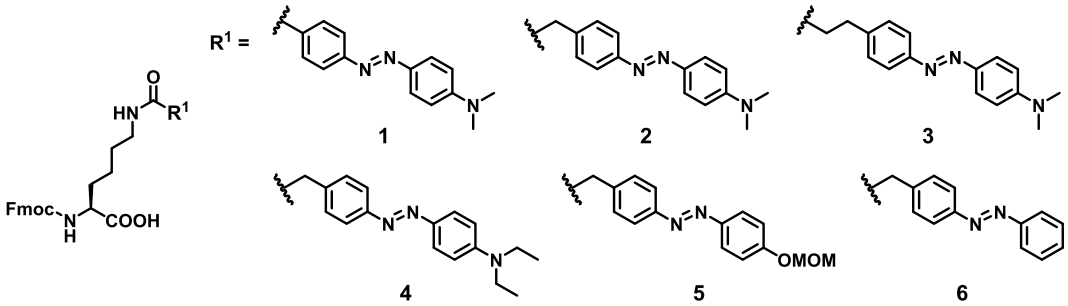

Scheme 1. Syntheses of Fmoc-Lys(Dabcyls)-OH 4, 5, and 6[a]

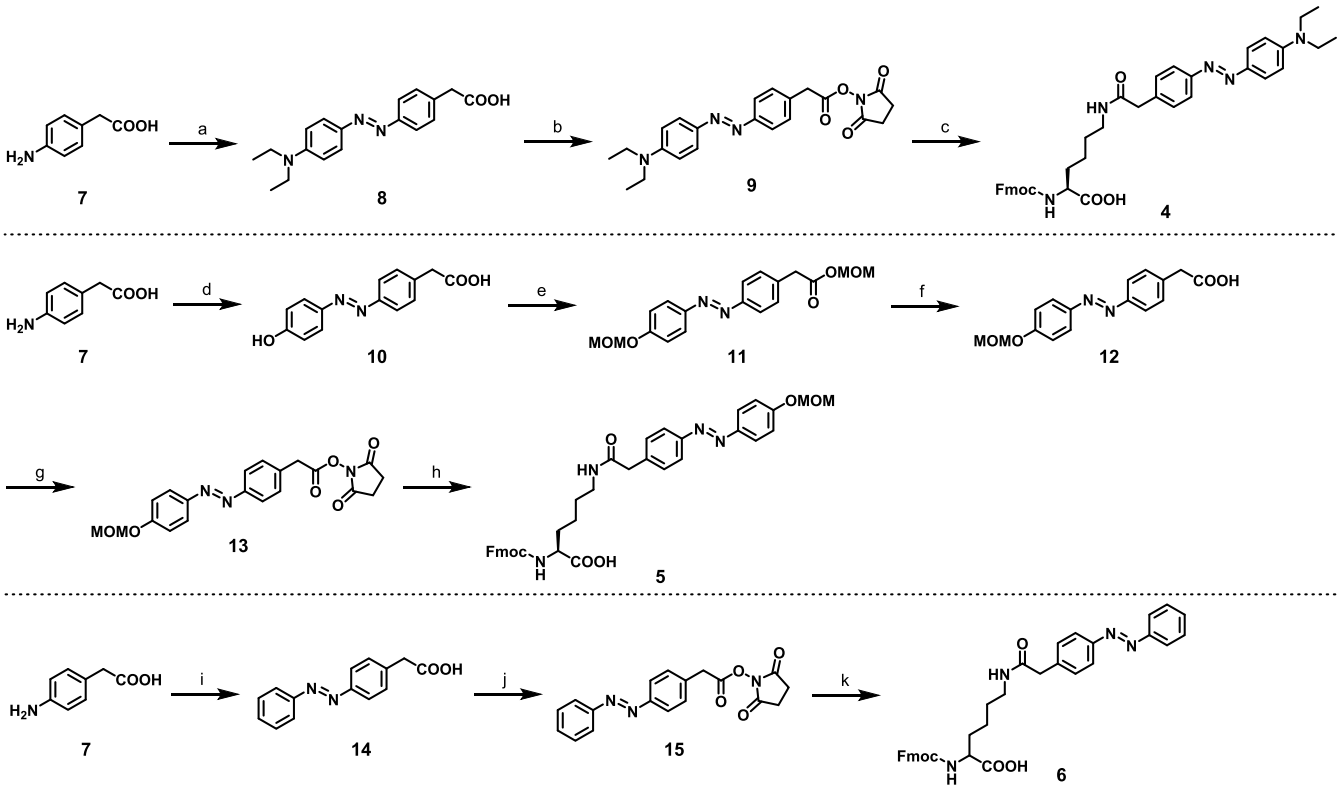

[a]Reagents and conditions: (a) $NaNO_2$, 1 N HCl, H_2O, 0 °C and then *N*,*N*-diethylaniline, H_2O/AcOH, 0 °C to room temperature (R.T.), 52%; (b) *N*-hydroxysuccinimide, EDCI·HCl, dimethylformamide (DMF), R.T., 9.2%; (c) Fmoc-Lys-OH·HCl, *N*,*N*-diisopropylethylamine (DIPEA), DMF, R.T., 35%; (d) $NaNO_2$, 1 N HCl, H_2O, 0 °C and then phenol, 2 N NaOH, 0 °C to R.T., 30%; (e) MOM-Cl, DIPEA, DMF, 0 °C to R.T., 86%; (f) 2 N NaOH, EtOH, 70 °C and then 2 N HCl, 69%; (g) *N*-hydroxysuccinimide, EDCI·HCl, DMF, R.T., 59%; (h) Fmoc-Lys-OH·HCl, DIPEA, DMF, R.T., 83%; (i) nitrosobenzene, AcOH, R.T., 90%; (j) *N*-hydroxysuccinimide, EDCI·HCl, DMF, R.T., 51%; and (k) Fmoc-Lys-OH·HCl, DIPEA, DMF, R.T., 86%.

inhibitors (**S2DMi-1−14**), as well as previously reported inhibitors, showed that the SIRT2-inhibitory activities evaluated with the two probes were strongly correlated with each other, whereas they were not correlated with the deacetylase-inhibitory activities. Thus, our fluorescence probe SFP3 can efficiently measure SIRT2 defatty-acylase activity. Interestingly, most of the previously reported inhibitors, including compound **TM** and SirReal2, showed only very weak SIRT2 defatty-acylase-inhibitory activity (IC_{50} > 2.0 and >10 μM, respectively),[19] whereas our newly synthesized inhibitors, **S2DMi-6**, **S2DMi-7**, and **S2DMi-9**, showed potent defatty-acylase-inhibitory activity (IC_{50} = 0.019−0.022 μM). Thus, the new inhibitors are expected to be useful as both research tools and candidate therapeutic agents.

CHEMISTRY

We first prepared dabcyl derivatives (**1**−**6**), whose carboxyl groups are linked to the ε-amino group of Fmoc-Lys-OH (Chart 1). Fmoc-Lys(Dabcyl)-OH (**1**), Fmoc-Lys(Dabcyl-EH)-OH (**2**), and Fmoc-Lys(Dabcyl-PH)-OH (**3**) were prepared as previously described.[29] The synthetic routes to **S2DMi-1−14** and their intermediates used in this study are shown in scheme 1−4. Scheme 1 shows the preparation of Fmoc-Lys(diEtDabcyl-EH)-OH (**4**), Fmoc-Lys(OH-Dabcyl-EH)-OH (**5**), and Fmoc-Lys(Dabcyl-EH-H)-OH (**6**). Azo coupling reaction between 4-aminobenzeneacetic acid (**7**) and *N*,*N*-diethylaniline or phenol afforded azobenzene **8** or **10**, respectively. Aminobenzeneacetic acid (**7**) was also coupled with nitrosobenzene to afford azobenzene **14**. The phenol

DOI: 10.1021/acs.jmedchem.9b00315
J. Med. Chem. XXXX, XXX, XXX−XXX

Scheme 2. Syntheses of S2DMi-1–8, S2DMi-13, and S2DMi-14[a]

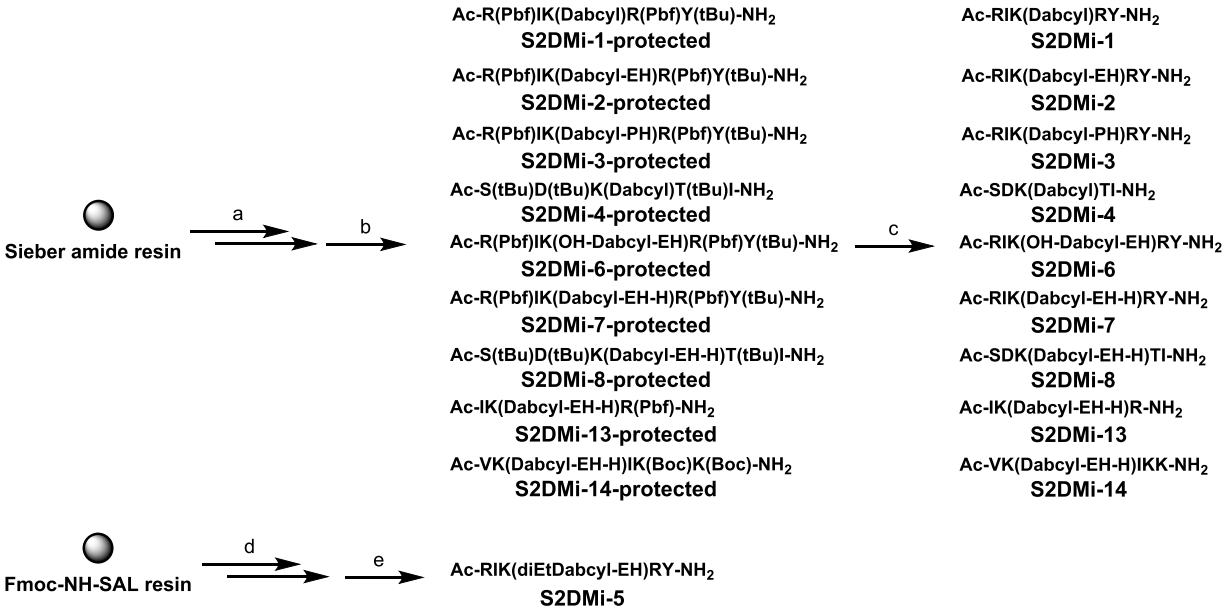

[a]Reagents and conditions: (a) Fmoc solid-phase synthesis using Sieber amide resin; (b) 1% TFA, 1% triethylsilane, CH_2Cl_2, R.T., 49% for **S2DMi-1-protected**, 82% for **S2DMi-2-protected**, 84% for **S2DMi-3-protected**, 64% for **S2DMi-4-protected**, 42% for **S2DMi-6-protected**, quant. for **S2DMi-7-protected**, 98% for **S2DMi-8-protected**, quant. for **S2DMi-13-protected**, 83% for **S2DMi-14-protected**; (c) 50% TFA, CH_2Cl_2, R.T., 65% for **S2DMi-1**, 79% for **S2DMi-2**, 874% for **S2DMi-3**, 42% for **S2DMi-4**, 22% for **S2DMi-6**, 60% for **S2DMi-7**, 39% for **S2DMi-8**, 58% for **S2DMi-13**, 30% for **S2DMi-14**; (d) Fmoc solid-phase synthesis using Fmoc-NH-SAL resin; and (e) 90% TFA, 5% H_2O, 5% triethylsilane, R.T., 11%.

Scheme 3. Synthesis of S2DMi-9[a]

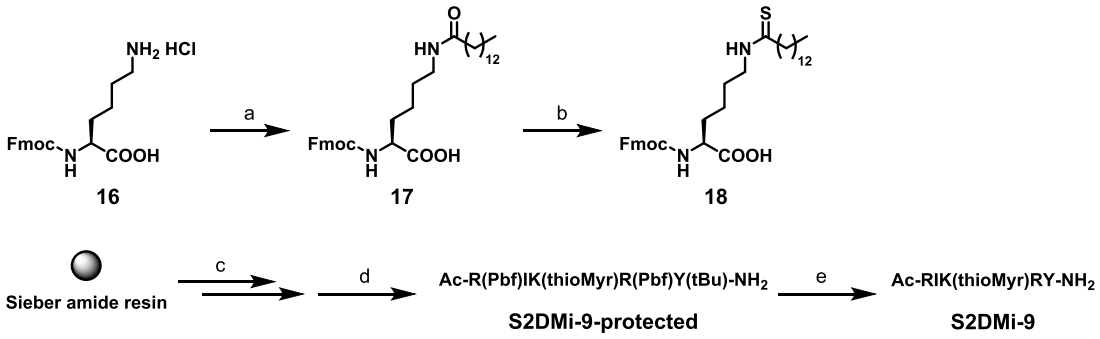

[a]Reagents and conditions: (a) myristoyl chloride, Na_2CO_3, dioxane, H_2O, 0 °C to R.T., 78%; (b) Lawesson's reagent, THF, R.T., 69%; (c) Fmoc solid-phase synthesis using Sieber amide resin; (d) 1% TFA, 1% triethylsilane, CH_2Cl_2, R.T., 99%; and (e) 50% TFA, CH_2Cl_2, R.T., 35%.

group of compound **10** was protected with methoxymethyl (MOM) to give compound **12** in two steps. The carboxyl groups of compounds **8**, **12**, and **14** were activated in the presence of *N*-hydroxysuccinimide and 1-ethyl-3-(3-dimethylaminopropyl)carbodiimide (EDCI) to afford succinimidyl ester compounds **9**, **13**, and **15**, respectively. Condensation reaction of each succinimidyl ester compound with the ε-amino group of Fmoc-Lys-OH gave the desired Fmoc-Lys(diEtDabcyl-EH)-OH (**4**), Fmoc-Lys(OH-Dabcyl-EH)-OH (**5**), and Fmoc-Lys(Dabcyl-EH-H)-OH (**6**).

Scheme 2 shows the syntheses of **S2DMi-1–8**, **S2DMi-13**, and **S2DMi-14**. Fmoc solid-phase synthesis using Sieber amide resin with modified lysine residues (**1–6**) gave protected **S2DMi-1–4**, **S2DMi-6–8**, **S2DMi-13**, and **S2DMi-14**. Protecting groups were removed by treatment with TFA. The crude peptides were purified by high-performance liquid chromatography (HPLC) to afford >95% pure **S2DMi-1–4**, **S2DMi-6–8**, **S2DMi-13**, and **S2DMi-14**. Fmoc solid-phase synthesis using Fmoc-NH-SAL resin also gave **S2DMi-5**.

The preparation of **S2DMi-9** is shown in Scheme 3. The amino group of Fmoc-Lys-OH was acylated with myristoyl chloride to afford compound **17**. The electron-rich amide group was converted to a thioamide group by using Lawesson's reagent to afford compound **18**. Fmoc solid-phase synthesis gave protected **S2DMi-9**, which was deprotected under acidic conditions to afford crude **S2DMi-9**. The crude peptide was purified by HPLC to afford **S2DMi-9**.

Scheme 4 illustrates the syntheses of **S2DMi-10–12**. Condensation of the amino group of Cbz-Lys-OH with azobenzene **13** gave compound **20**. Compound **20** was condensed with H-Ala-NH_2 in the presence of COMU to afford compound **21**. Removal of the MOM group of compound **21** under acidic conditions gave **S2DMi-10**.

DOI: 10.1021/acs.jmedchem.9b00315
J. Med. Chem. XXXX, XXX, XXX–XXX

Scheme 4. Syntheses of S2DMi-10−12[a]

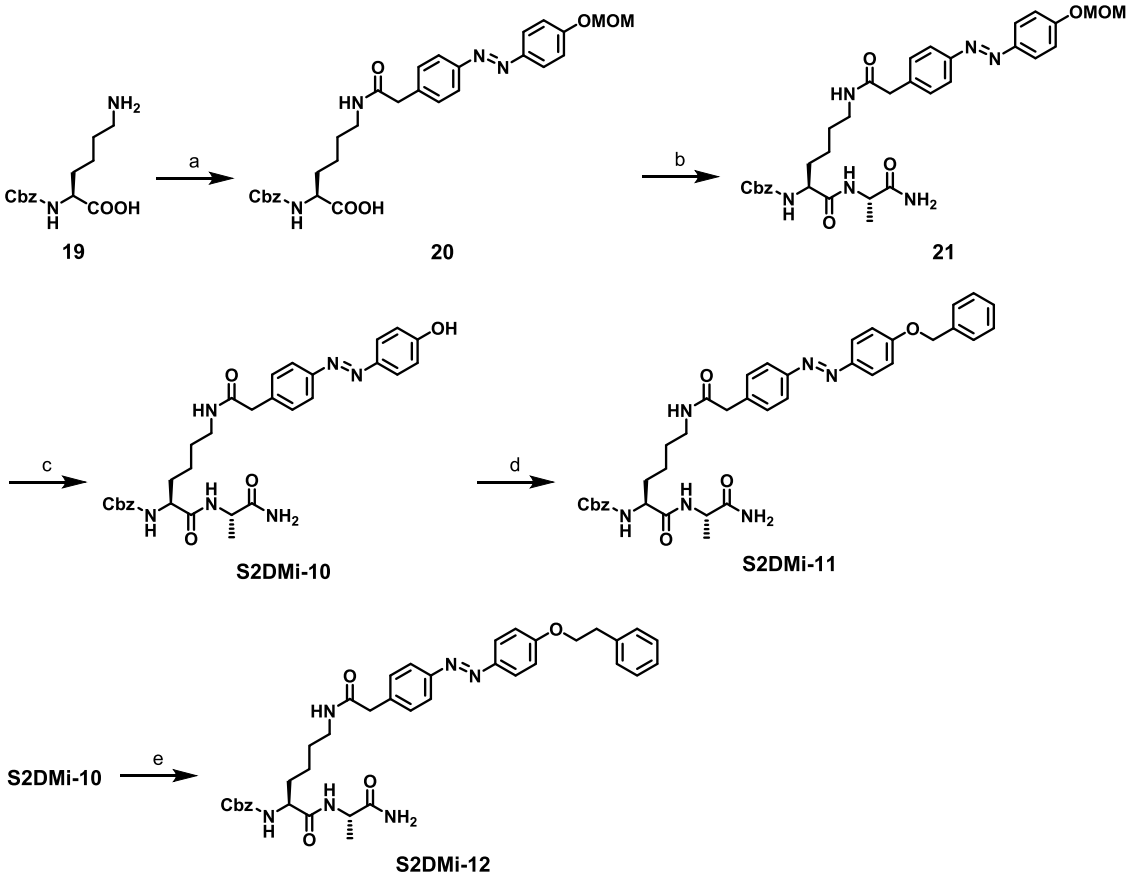

[a]Reagents and conditions: (a) **13**, DIPEA, DMF, R.T., 74%; (b) H-Ala-NH_2·HCl, (1-cyano-2-ethoxy-2-oxoethylidenaminooxy)dimethylamino-morpholino-carbenium hexafluorophosphate (COMU), DIPEA, DMF, R.T., 84%; (c) 50% trifluoroacetyl (TFA), CH_2Cl_2, R.T., 76%; (d) benzyl bromide, Cs_2CO_3, tetrabutylammonium iodide (TBAI), DMF, R.T., 84%; and (e) phenethyl bromide, Cs_2CO_3, TBAI, DMF, R.T., 42%.

Alkylation of **S2DMi-10** with benzyl bromide or phenethyl bromide gave **S2DMi-11** or **S2DMi-12**, respectively.

The preparation of **p53(Myr)-AMC** is shown in Scheme 5. Condensation of the carboxyl group of Cbz-Lys(Boc)-OH with 7-amino-4-methylcoumarin (**22**) gave compound **23**. The Boc group was removed by the treatment with TFA, and the formed amino group was condensed with myristoyl chloride to afford compound **25**. The Cbz group was removed by catalytic reduction using Pd/C under H_2, and the formed amino group was condensed with Ac-Arg(Pbf)-His(Trt)-Lys(Boc)-OH tripeptide (**29**) to afford compound **27**. Protecting groups were removed by treatment with TFA, and the crude peptide was purified by HPLC to afford >95% pure **p53(Myr)-AMC**.

Scheme 6 illustrates the syntheses of **H4K16-NH_2**, **H4K16-Ac**, and **H4K16-Myr**. Fmoc solid-phase synthesis using the Sieber amide resin with Boc-protected, acetylated, or myristoylated lysine residues gave protected **H4K16-NH_2**, **H4K16-Ac**, and **H4K16-Myr**. Protecting groups were removed by treatment with TFA. The crude peptides were purified by HPLC to afford >95% pure **H4K16-NH_2**, **H4K16-Ac**, and **H4K16-Myr**.

RIK^{Tfa}RY and compounds **M** and **TM** were synthesized in accordance with the previous reports.[28,19]

RESULTS

We previously reported a fluorescence resonance energy transfer-based fluorescence probe, SFP3, designed to establish a one-step sirtuin activity probe.[29] As shown in Figure 1a, SFP3 consists of fluorescein, H3K9 peptide, and dabcyl propanoic acid (Dabcyl-PH) quencher attached to the ε-amino group of the lysine residue. In the presence of sirtuin and NAD^+, Dabcyl-PH of SFP3 is cleaved by SIRT1−3 and 6, affording a strongly fluorescent product, SFP0. Recently, Jung and co-workers reported that SIRT2 has a unique "selectivity pocket".[20] Here, we hypothesized that the hydrophobic Dabcyl quencher and long-chain fatty acyl groups are both recognized by the same selectivity pocket of SIRT2 (Figure 1b). If this is the case, the Dabcyl moiety might compete with long-chain fatty acyl groups for binding to the selectivity pocket, that is, it might be a specific competitive inhibitor of SIRT2 defatty-acylase activity. Thus, we anticipated that SFP3 might efficiently measure the defatty-acylase activity of SIRT2. To test these ideas, we synthesized a series of new peptide-based SIRT2 inhibitors bearing a Dabcyl moiety and evaluated their SIRT2-inhibitory activity by means of the SFP3 assay.

In designing the new compounds, we were concerned that the Dabcyl-PH group might be cleaved by SIRT2, as in the case of SFP3 (Figure 1a). As our previously reported fluorescence probes SFP1 and SFP2, which contain Dabcyl and Dabcyl-EH, respectively, instead of the Dabcyl-PH moiety in SFP3, were unreactive to SIRT2,[29] we focused on Dabcyl or Dabcyl-EH instead of Dabcyl-PH to decrease the electron density of the amide group with the aim of making the compounds inert to SIRT2-mediated cleavage (Figure 1c).

DOI: 10.1021/acs.jmedchem.9b00315
J. Med. Chem. XXXX, XXX, XXX−XXX

Scheme 5. Synthesis of p53(Myr)-AMC[a]

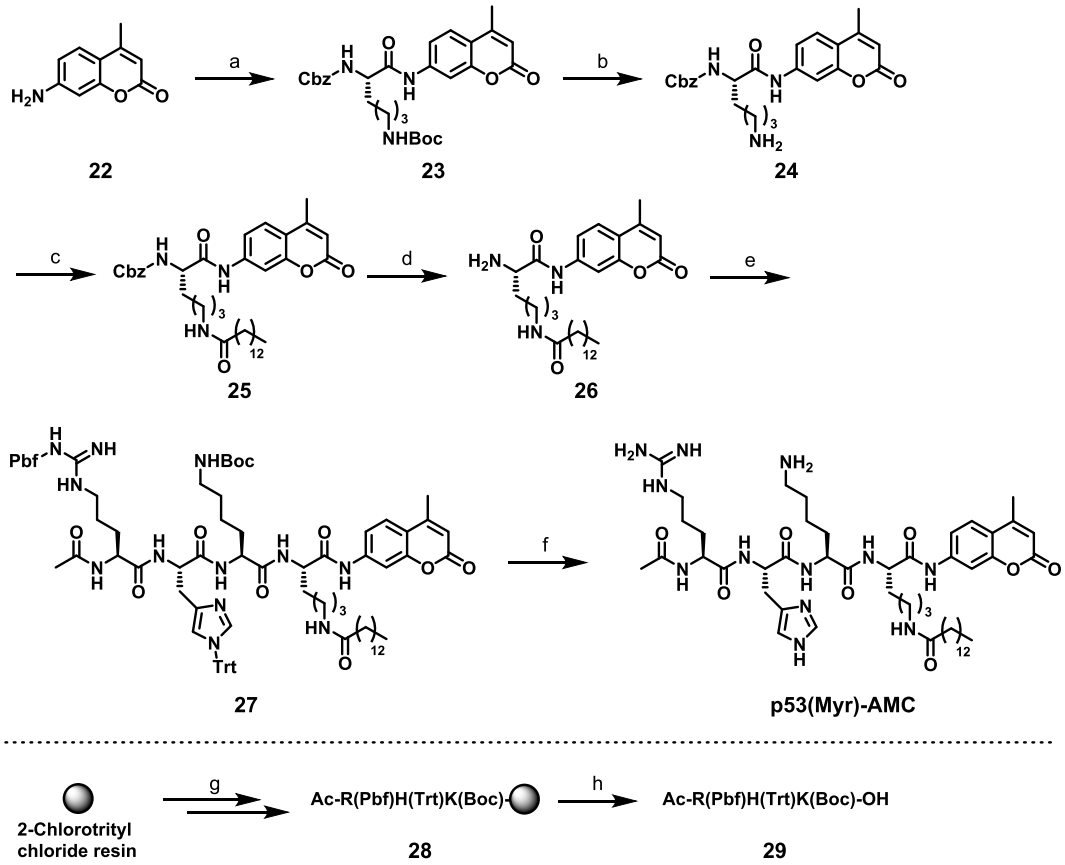

[a]Reagents and conditions: (a) Cbz-Lys(Boc)-OH, COMU, DIPEA, DMF, R.T., 38%; (b) 50% TFA, CH_2Cl_2, R.T., 77%; (c) myristoyl chloride, DIPEA, CH_2Cl_2, R.T., 75%; (d) Pd/C, H_2, MeOH, CH_2Cl_2, R.T., quant.; (e) **29**, COMU, DIPEA, DMF, R.T, 70%; (f) TFA, CH_2Cl_2, R.T., 58%; (g) Fmoc solid-phase synthesis using 2-chlorotrityl chloride resin; and (h) 1% TFA, CH_2Cl_2, 87%.

Scheme 6. Syntheses of H4K16-NH_2, H4K16-Ac, and H4K16-Myr[a]

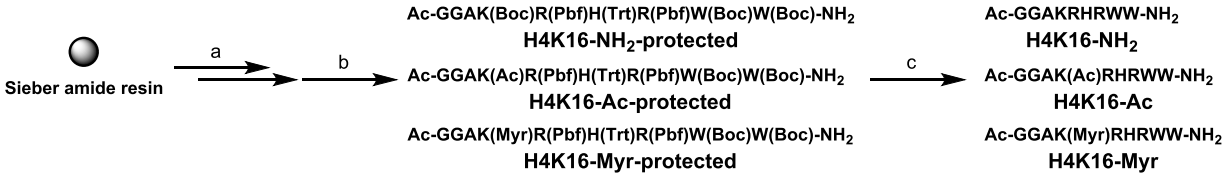

[a]Reagents and conditions: (a) Fmoc solid-phase synthesis using Sieber amide resin; (b) 1% TFA, 1% triethylsilane, CH_2Cl_2, R.T., quant. for **H4K16-NH_2-protected**, 98% for **H4K16-Ac-protected**, and 95% for **H4K16-Myr-protected**; (c) 50% TFA, CH_2Cl_2, R.T., 61% for **H4K16-NH_2**, 70% for **H4K16-Ac**, and 65% for **H4K16-Myr**.

Thus, we designed and synthesized **S2DMi-1−14**, which contain Ac-Arg-Ile-Lys-Arg-Tyr-NH_2 (Ac-RIKRY-NH_2), Ac-Ser-Asp-Lys-Thr-Ile-NH_2 (Ac-SDKTI-NH_2), or Cbz-KA-NH_2, in which the ε-amino group of lysine is acylated by Dabcyl, Dbcyl-EH, or Dabcyl-PH, or a thiomyristoyl group (Chart 2). We also prepared **RIK^{Tfa}RY** as a reference compound (Chart 2).[28] We examined the SIRT2-inhibitory activity by using SFP3 as a substrate and found that **RIK^{Tfa}RY**, **S2DMi-1**, and **S2DMi-3** showed moderate SIRT2-inhibitory activity (Table 1, IC_{50} = 0.32, 0.43, and 0.30 μM, respectively), whereas **S2DMi-2** showed about 9-fold stronger inhibitory activity (IC_{50} = 0.036 μM) than **RIK^{Tfa}RY**. Thus, the Dabcyl-EH scaffold appears to be suitable as a SIRT2-inhibitory core structure. We next checked the stability of **S2DMi-1−3** in the presence of SIRT2 and NAD^+. HPLC analysis showed that **S2DMi-1** and **S2DMi-3** afforded complex degradation together with deacylation products, Dabcyl and Dabcyl-PH, respectively (Figure 2a,e), whereas **S2DMi-2** was stable, remaining >99% intact after 4 h incubation (Figure 2c). We next examined the time dependence of the SIRT2-inhibitory activity of **S2DMi-1−3**. The inhibitory activities of **S2DMi-1** and **S2DMi-3** toward SIRT2 decreased time-dependently (Figure 3b,f), whereas that of **S2DMi-2** remained nearly constant for 60 min (Figure 2d), in accordance with the HPLC analyses. These results confirm that the phenylacetyl group of Dabcyl-EH is resistant to deacylation by SIRT2 and thus should be suitable for use as an inhibitory core structure.

We next evaluated **S2DMi-4−14**, together with known SIRT2 inhibitors, including compound **M**, compound **TM**, AGK2, nicotinamide (NAM), and SirReal2 (Chart 2) in the SFP3 assay. **S2DMi-5−7** all showed potent inhibitory activities (Table 1, IC_{50} = 0.068, 0.019, and 0.019 μM, respectively). In

DOI: 10.1021/acs.jmedchem.9b00315
J. Med. Chem. XXXX, XXX, XXX−XXX

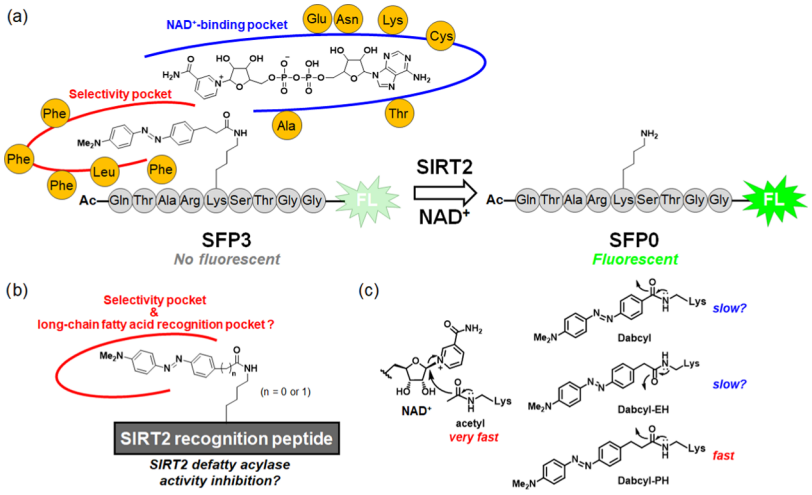

Figure 1. (a) Schematic illustration of our hypothesis that the Dabcyl-PH group of our sirtuin fluorescence probe SFP3 is accommodated in the SIRT2 selectivity pocket and is cleaved by SIRT2 defatty-acylase activity. (b) Design of SIRT2 defatty-acylase inhibitors with a SIRT2 recognition peptide and cleavage-resistant Dabcyl and Dabcyl-EH moieties. (c) The relative rate of reaction of the acylated amino group of lysine with NAD^+ in the SIRT2 catalytic pocket is expected to depend on the electron density of the amide group.

contrast, **S2DMi-4** and **S2DMi-8**, which contain the SDKTI peptide instead of RIKRY in **S2DMi-1** and **S2DMi-7**, showed about 80-fold weaker inhibitory activity (IC_{50} = >2.0 and 1.5 μM, respectively), suggesting that the peptide sequence is critical for SIRT2 inhibition. **S2DMi-9**, which has a thiomyristolated lysine peptide, showed similar inhibitory activity (IC_{50} = 0.022 μM) to **S2DMi-6** and **S2DMi-7**, suggesting that it acts as a mechanism-based inhibitor. However, the thiomyristoyl group of **S2DMi-9** is expected to form a covalent bond with NAD^+ resulting in strong and lasting inhibition, whereas **S2DMi-6**, **S2DMi-7**, and **S2DMI-9** are expected to have a different inhibitory mechanism. This speculation was supported by the results of HPLC analyses and examination of the time dependence of inhibitory activity. Indeed, while HPLC analysis showed that **S2DMi-6** and **S2DMi-9** were both stable in the presence of SIRT2 and NAD^+ (Figure 2g,i), their SIRT2-inhibitory characteristics were different. That is, the inhibitory activity of **S2DMi-6** was essentially constant (Figure 2h), whereas that of **S2DMi-9** increased time-dependently (Figure 2j), suggesting the accumulation of the **S2DMi-9**−NAD^+ complex. On the other hand, **S2DMi-10**−**12** showed very weak inhibitory activities in spite of having the Dabcyl-EH scaffold, like **S2DMi-6**. Surprisingly, compound **TM**, a selective and potent SIRT2 inhibitor, showed almost no inhibitory activity toward SIRT2 in the SFP3 assay. These results suggest that the peptide sequences Cbz-Lys-Ala-NH_2 (**S2DMi-10**−**12**) and Cbz-Lys (compound **M** and **TM**) are not suitable for inhibiting SIRT2-mediated SFP3 cleavage. This idea is supported by the results for **S2DMi-13** and **14**, which have truncated (Ac-Ile-Lys-Arg-NH_2) and K-Ras4a peptide (Ac-Val-Lys-Ile-Lys-Lys-NH_2) sequences with the phenylacetyl scaffold, like **S2DMi-7**;[16] these compounds exhibited weaker inhibitory activities than **S2DMi-7** (IC_{50} = 0.063 and 0.12 μM, respectively). In addition, compound **6** (Chart 1) itself exhibited no inhibitory activity toward SIRT2, suggesting that the Dabcyl-EH scaffold is not sufficient for SIRT2 inhibition (Figure S5). Thus, the RIKRY sequence was considered to be the most suitable peptide among those examined. Finally, the known SIRT2 inhibitors AGK2 and SirReal2 showed almost no inhibitory activity in the SFP3 assay (IC_{50} > 50 and >10 μM, respectively), though NAM showed moderate inhibitory activity (IC_{50} = 11 μM); this is consistent with the fact that NAM is a common byproduct of both deacetylation and deacylation mediated by SIRT2.

Since compound **TM**, AGK2, and SirReal2 are reported to be potent SIRT2 deacetylase inhibitors (IC_{50} = 0.028, 3.5, and 0.14 μM, respectively),[19,21] but exhibited very weak inhibitory activity in the SFP3 assay, the activity evaluated by SFP3 is likely to be distinct from the SIRT2 deacetylase activity. Therefore, we hypothesized that the enzymatic activity detected by SFP3 is SIRT2's defatty-acylase activity. To confirm this, we synthesized **p53(Myr)-AMC** as another demyristoylase fluorescence probe (Figure 3a). **p53(Myr)-AMC** was hydrolyzed by SIRT2, releasing p53(NH_2)-AMC (Figure 3b), and the SIRT2 demyristoylase activity could be detected in terms of a fluorescence increment upon subsequent enzymatic reaction with trypsin (Figure 3a,c). Thus, we used **p53(Myr)-AMC** to evaluate the SIRT2 demyristoylase-inhibitory activity of the above compounds and reported inhibitors. **S2DMi-2**, **S2DMi-5**−**7**, **S2DMi-9**, **S2DMi-13**, and **S2DMi-14** were potent/moderate SIRT2 demyristoylase inhibitors (Table 1, IC_{50} = 0.13, 0.19, 0.044, 0.051, 0.044, 0.25, and 0.52 μM, respectively), whereas other **S2DMis** were weak inhibitors (IC_{50} > 1.1 μM). Compounds **M**, **TM**, and AGK2 showed almost no inhibitory activity, though NAM was inhibitory (IC_{50} = 20 μM). The IC_{50} values obtained with **p53(Myr)-AMC** were strongly correlated to those obtained with SFP3 (correlation coefficient: 0.993 (Figure 4a)). The finding that the activity evaluated by the SFP3 assay well reflects the demyristoylase activity of SIRT2 strongly supports our above hypothesis, indicating that SFP3 is available as a specific activity probe for SIRT2 defatty-acylase activity.

In addition, we measured the inhibitory activities of the above compounds toward the enzymatic reaction of SIRT2 with **H4K16-Myr** and **H4K16-Ac** peptides, which is similar to a native SIRT2 substrate, lacking a fluorophore. **S2DMi-6**, **S2DMi-7**, and **S2DMi-9** inhibited the demyristoylation reaction in a dose-dependent manner, whereas compound **TM**, AGK2, and SirReal2 showed no demyristoylation-inhibitory activity (Figures 5 and S5). These results are consistent with those in the SFP3 and **p53(Myr)-AMC** assays.

DOI: 10.1021/acs.jmedchem.9b00315
J. Med. Chem. XXXX, XXX, XXX−XXX

Chart 2. Structures of Candidate SIRT2 Defatty-acylase Inhibitors Synthesized in This Study (S2DMi-1−14) and Reported SIRT2 Inhibitors, Compounds M, TM, AGK2, Nicotinamide (NAM), and SirReal2[a]

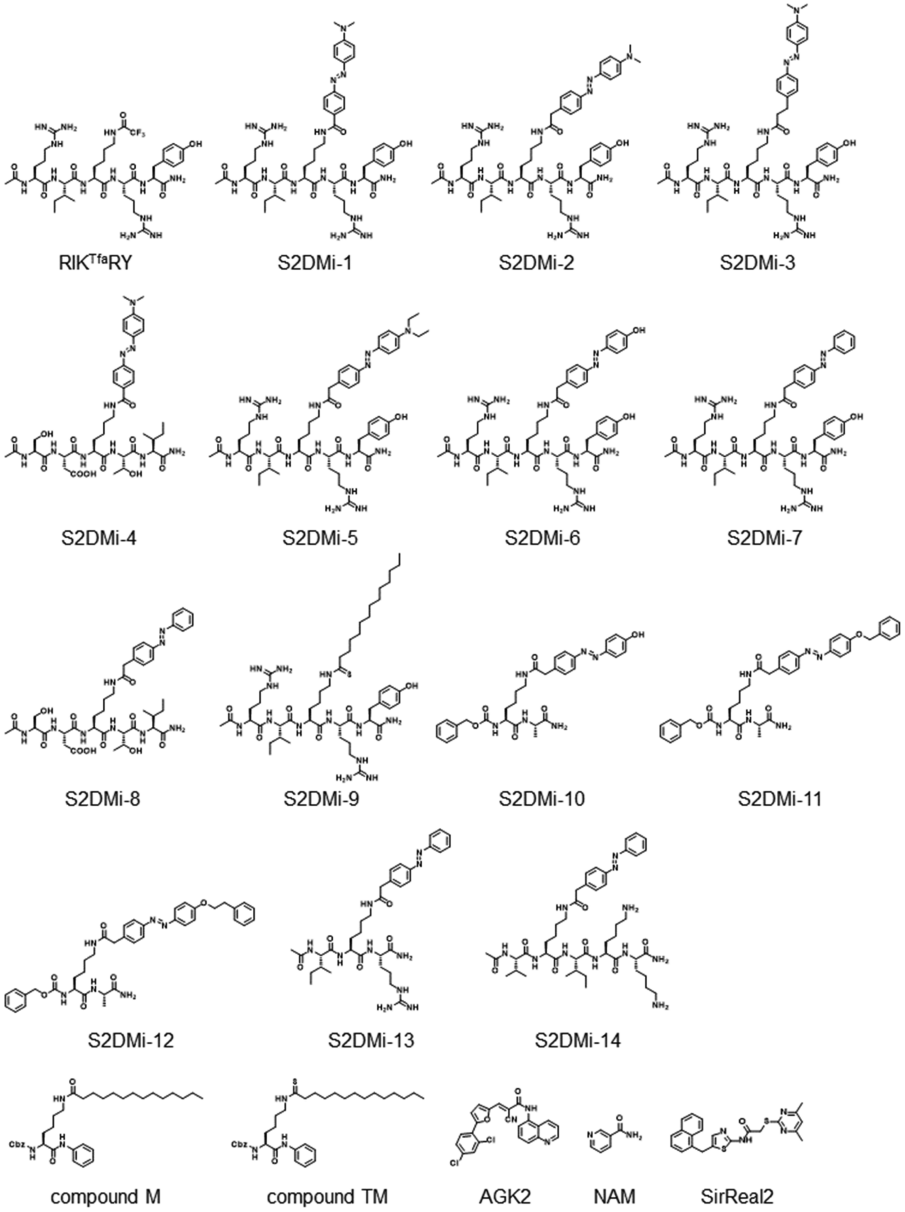

[a]Absorption spectra of these compounds are shown in Figure S1.

Although the inhibitory activities of **S2DMi-6**, **S2DMi-7**, and **S2DMi-9** were weaker than in SFP3 and **p53(Myr)-AMC** assays, this may be at least partly because the concentrations of **H4K16-Myr** (SIRT2 substrate) and SIRT2 were much higher. Overall, these results demonstrate that **S2DMi-6**, **S2DMi-7**, and **S2DMi-9** inhibited SIRT2 demyristoylase activity, whereas reported SIRT2 inhibitors, including compound **TM**, AGK2, and SirReal2, did not affect this activity even in the assay with the native peptide substrate.

Next, we tried to directly compare the SIRT2 deacetylase and demyristoylase-inhibitory activities of **S2DMi-6**, **S2DMi-7**, and **S2DMi-9** by utilizing the **H4K16-Ac** peptide. In the result, it was found that **S2DMi-6**, **S2DMi-7**, and **S2DMi-9** inhibited the deacetylation reaction more potently than the demyristoylation reaction in a dose-dependent manner (Figure S7). We speculate that this result is due to the difference of K_m values of two peptide substrates, **H4K16-Ac** and **H4K16-Myr** (K_m = 21.1 and 0.202 μM for **H4K16-Ac** and **H4K16-Myr**, respectively; Figure S8), meaning that much higher concentrations of **S2DMi-6**, **S2DMi-7**, and **S2DMi-9** are necessary to inhibit the SIRT2 demyristoylase activity because **H4K16-Myr** can bind with SIRT2 more tightly than **H4K16-Ac**.

We further tested the SIRT2 deacetylase-inhibitory activity of the above compounds by using the commercially available FLUOR DE LYS SIRT2 assay kit. **RIK^{Tfa}RY**, compound **M**, AGK2, and SirReal2 showed potent to moderate SIRT2-inhibitory activities, corresponding well with the reported values (Table 1, IC_{50} = 0.067, 0.14, 8.9, and 0.70 μM, respectively).[19−21] **S2DMi-1−14** exhibited moderate SIRT2-inhibitory activities (IC_{50} = 0.11−1.2 μM), which were weaker than those in the SFP3 assay. Notably, the IC_{50} values in the FLUOR DE LYS assay and the SFP3 assay showed no

DOI: 10.1021/acs.jmedchem.9b00315
J. Med. Chem. XXXX, XXX, XXX−XXX

Table 1. SIRT2-Inhibitory Activities (IC_{50}) and/or % Inhibition Values of RIK^{Tfa}RY, S2DMi-1−14, Compounds M, TM, AGK2, Nicotinamide (NAM), and SirReal2 Evaluated by Using SFP3, p53(Myr)-AMC (deMyr), and FLUOR DE LYS SIRT2 Assay Kits (deAc)[g]

	SIRT2 (μM) SFP3	SIRT2 (μM) deMyr	SIRT2 (μM) deAc
RIK^{Tfa}RY	0.32 ± 0.030	1.1 ± 0.14	0.067 ± 0.006, 0.031[c]
S2DMi-1	0.43 ± 0.023	1.6 ± 0.46	1.6 ± 0.44
S2DMi-2	0.036 ± 0.006	0.13 ± 0.021	0.17 ± 0.022
S2DMi-3	0.30 ± 0.022	>2.0, 23%[b]	1.1 ± 0.11
S2DMi-4	>2.0, 7.8%[a]	>2.0, 2.0%[b]	1.2 ± 0.10
S2DMi-5	0.068 ± 0.007	0.19 ± 0.020	0.26 ± 0.020
S2DMi-6	0.019 ± 0.007	0.044 ± 0.005	0.11 ± 0.011
S2DMi-7	0.019 ± 0.006	0.051 ± 0.006	0.18 ± 0.013
S2DMi-8	1.5 ± 0.10	>2.0, 17%[b]	0.58 ± 0.038
S2DMi-9	0.022 ± 0.003	0.044 ± 0.004	0.11 ± 0.013
S2DMi-10	>2.0, 18%[a]	5.3%[b]	0.19 ± 0.013
S2DMi-11	>2.0, 13%[a]	3.2%[b]	0.19 ± 0.020
S2DMi-12	>2.0, 1.4%[a]	>2.0, 2.9%[b]	0.40 ± 0.024
S2DMi-13	0.063 ± 0.008	0.25 ± 0.020	0.11 ± 0.010
S2DMi-14	0.12 ± 0.011	0.52 ± 0.068	0.12 ± 0.015
compound **M**	>2.0, 2.8%[a]	5.2%[b]	>1.0, 42%[b]
compound **TM**	>2.0, 4.2%[a]	4.2%[b]	0.14 ± 0.014, 0.028[d]
AGK2	>50	>50	8.9 ± 2.3, 3.5[e]
NAM	11 ± 1.6	20 ± 2.2	38 ± 1.8
SirReal2	>10	>10	0.70 ± 0.061, 0.14[f]

[a]Inhibition (%) at 2 μM. [b]Inhibition (%) at 1 μM. [c]Data from ref 28. [d]Data from ref 19. [e]Data from ref 21. [f]Data from ref 20. [g]The data indicate IC_{50} (mean ± standard deviation (S.D.), n = 3) of at least two experiments. For details, see Figures S2−S4.

correlation (correlation coefficient: 0.135 (Figure 4b)), suggesting that these two catalytic activities of SIRT2 are independent and that SFP3 can efficiently measure defatty-acylase activity of SIRT2. None of the compounds tested showed inhibitory activity toward Developer II solution (Figure S14), indicating that the inhibitory activities in the FLUOR DE LYS assay represent SIRT2 deacetylase-inhibitory activities.

To examine the selectivity of the above compounds, we evaluated their inhibitory activities toward SIRT1, 3, and 6 by using the SFP3 assay. The potent inhibitors of the SIRT2 defatty-acylase activity, such as **S2DMi-2**, **S2DMi-5−7**, **S2DMi-9**, **S2DMi-13**, and **S2DMi-14**, also showed moderate/potent inhibitory activities toward SIRT1 (Table 2) and SIRT3 (Table 2). In contrast, these inhibitors, except **S2DMi-9**, exhibited much weaker inhibitory activity toward SIRT6 (Table 2). We also evaluated the inhibitory activities toward SIRT1 and 3 demyristoylase activities by using **p53(Myr)-AMC** because it was found that **p53(Myr)-AMC** can detect SIRT1 and SIRT3 demyristoylase activities in the same manner as SIRT2 (Figure S15). **S2DMi-2**, **S2DMi-5−7**, **S2DMi-9**, **S2DMi-13**, and **S2DMi-14** also potently inhibited SIRT1 and 3 demyristoylase activities, and their inhibitory activities were similar to those obtained in the SFP3 assay (Table 2). It was surprising that the synthesized inhibitors showed little selectivity for SIRT2 over other SIRTs, even though they contained the SIRT2-selective peptide sequence RIKRY.[28] It is possible that the binding of fatty-acylated peptide induces a conformational change that alters the substrate recognition. This is plausible because binding of a thiomyristoylated peptide, BHJH-TM1, with SIRT2 induced a substantial conformational change.[12] It was also suggested that the structures of the hydrophobic pockets of SIRT1−3 are quite similar, but different from that of SIRT6, which seems consistent with the results in Table 2.

We examined whether **S2DMi-6**, **S2DMi-7**, and **S2DMi-9** permeate the cell membrane and inhibit sirtuin activities in cells. For such purposes, we set out to evaluate HeLa cells viability because it is reported that SIRT2-selective inhibitors, such as compound **TM**, inhibit HeLa cells growth via a degradation of c-Myc protein, which is associated with SIRT2 deacetylation activity.[19] In addition, it was found that **S2DMi-6**, **S2DMi-7**, and **S2DMi-9** strongly inhibit SIRT2 deacetylase activity, and their activities are almost the same as that of compound **TM** (Table 1). Cell viability assay showed that **S2DMi-6**, **S2DMi-7**, and **S2DMi-9** did not inhibit cell growth even at 50 μM; in contrast, compound **TM** strongly inhibited cell growth, which is consistent with the previous report (Figure S16).[19] This result suggests that **S2DMi-6**, **S2DMi-7**, and **S2DMi-9** cannot permeate the cell membrane or they are unstable in cellular systems.

We finally set out to elucidate the inhibition mechanism of **S2DMi-6** and **S2DMi-9**. Michaelis−Menten and Lineweaver−Burk plots indicated that **S2DMi-6** and **S2DMi-9** show mixed inhibition of SIRT2-mediated hydrolysis of SFP3 (Figure 6). In contrast, **S2DMi-6** and **S2DMi-9** showed noncompetitive inhibition with respect to NAD^+ (Figures 6 and S17).

■ DISCUSSION AND CONCLUSIONS

Our results here show that our previously reported fluorescence probe SFP3 can efficiently measure the defatty-acylase activity of SIRT2. The inhibitory activities of the synthesized inhibitors in the SFP3 assay were strongly correlated with those toward **p53(Myr)-AMC**, which can monitor SIRT1−3 demyristoylase activities. Importantly, the SIRT2 defatty-acylase-inhibitory activities of the synthesized compounds were not correlated with their SIRT2 deacetylase-inhibitory activities, suggesting that these two enzymatic activities are independent of each other. Notably, most previously reported inhibitors, except **RIK^{Tfa}RY**, showed

DOI: 10.1021/acs.jmedchem.9b00315
J. Med. Chem. XXXX, XXX, XXX−XXX

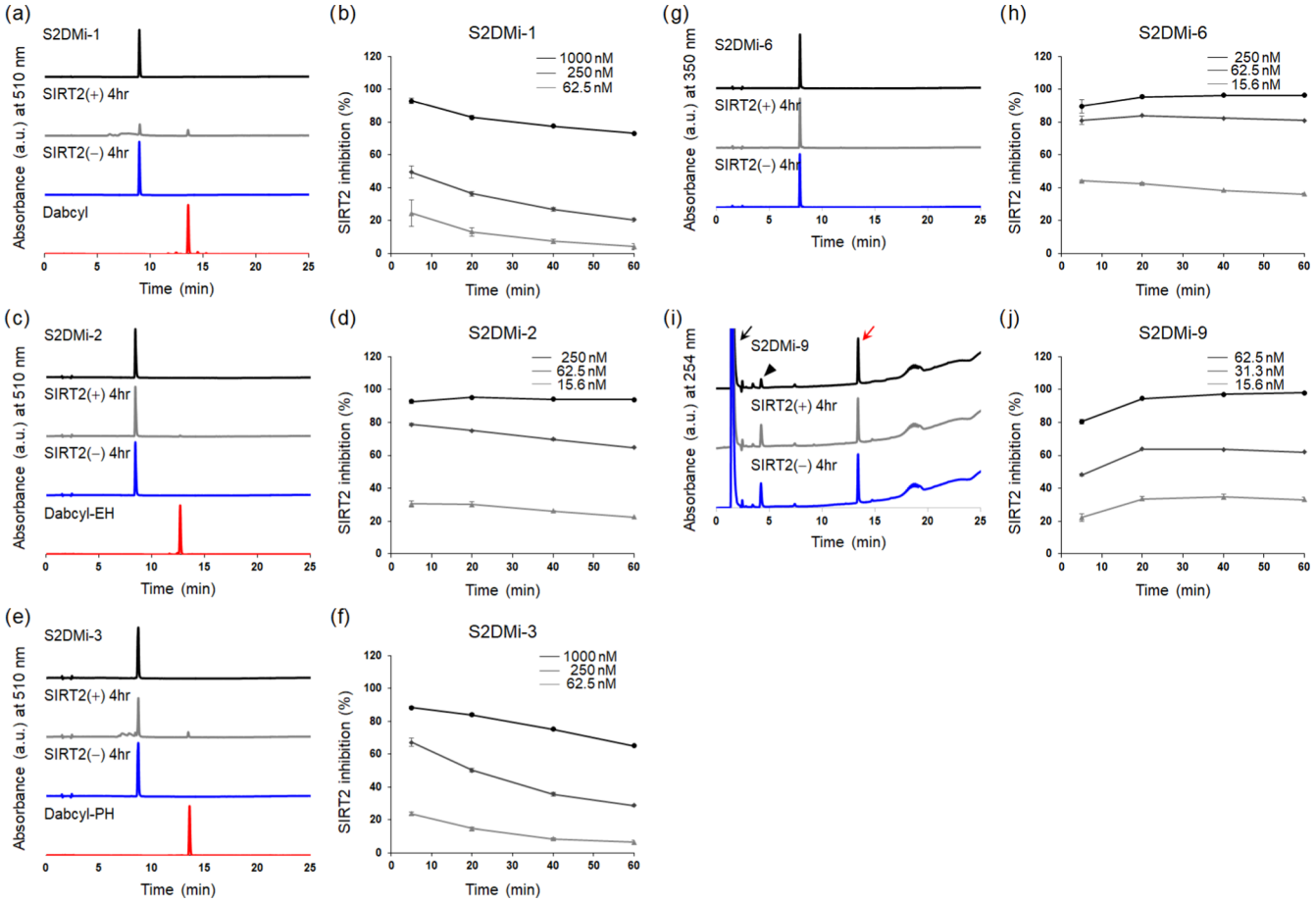

Figure 2. (a, c, e, g, i) HPLC stability analyses of 20 μM **S2DMi-1−3**, **S2DMi-6**, and **S2DMi-9** in the presence or absence of 350 nM SIRT2 and 500 μM NAD^+ for 4 h at 37 °C. Reactions were performed in SIRT assay buffer I (50 mM Tris−HCl (pH 8.0), 150 mM NaCl, 1 mM dithiothreitol (DTT), and 0.05% Triton X-100), containing 0.2% dimethyl sulfoxide (DMSO). HPLC conditions: A/B = 80:20 (initial) → 0:100 (20 min) → 0:100 (23 min) with a linear gradient, A = 0.1% TFA Milli-Q, B = 0.1% TFA CH_3CN. In (i), a red arrow, a black arrow, and an arrowhead indicate **S2DMi-9**, NAD^+, and DTT, respectively. Absorbance was monitored at 510 nm (**S2DMi-1−3**), 350 nm (**S2DMi-6**), or 254 nm (**S2DMi-9**). (b, d, f, h, j) Time dependence of SIRT2-inhibitory activities of **S2DMi-1−3**, **S2DMi-6**, and **S2DMi-9** (indicated concentrations). The results are shown as mean ± S.D. (n = 3).

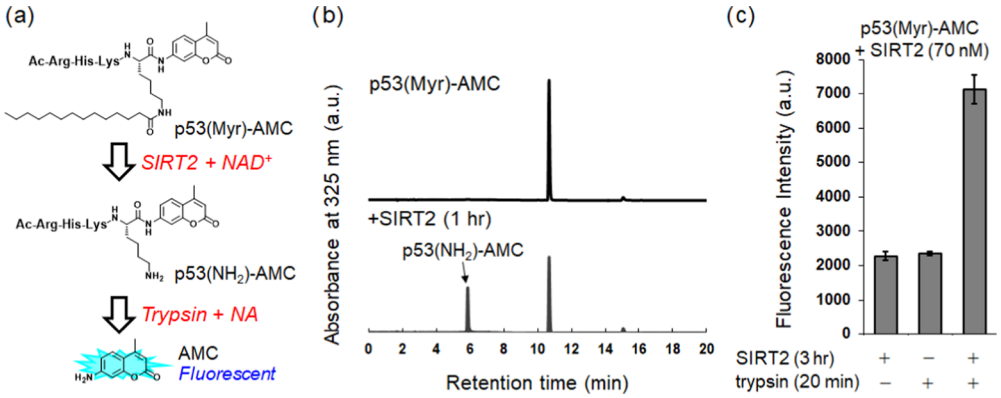

Figure 3. (a) Application of **p53(Myr)-AMC** fluorescence probe for measuring SIRT2 demyristoylase activity. (b) HPLC analyses of enzymatic reactions of 50 μM **p53(Myr)-AMC** and 500 μM NAD^+ with 175 nM SIRT2 after 1 h. Absorbance at 325 nm was monitored. (c) Enzymatic reactions were performed in 50 μM **p53(Myr)-AMC** and 500 μM NAD^+ with or without 70 nM SIRT2 for 3 h, and then 1 mM NAM and 100 nM trypsin were added. Fluorescence intensity (F.I.) was measured with an ARVO X5 plate reader (filters: Ex = 355/40 nm, Em = 460/25 nm) for 20 min at 37 °C. The results are shown as mean ± S.D. (n = 3).

almost no SIRT2 defatty-acylase-inhibitory activity. Therefore, our compounds, such as **S2DMi-6**, **S2DMi-7**, and **S2DMi-9**, are the first potent SIRT2 defatty-acylase inhibitors, having IC_{50} values of nM order; however, they inhibit SIRT2 deacetylase activity more potently than the demyristoylase one from the native-peptide-based assay (Figures 5 and S7), whose characteristics are needed to be improved in the future to develop SIRT defatty-acylase-specific inhibitors.

DOI: 10.1021/acs.jmedchem.9b00315
J. Med. Chem. XXXX, XXX, XXX−XXX

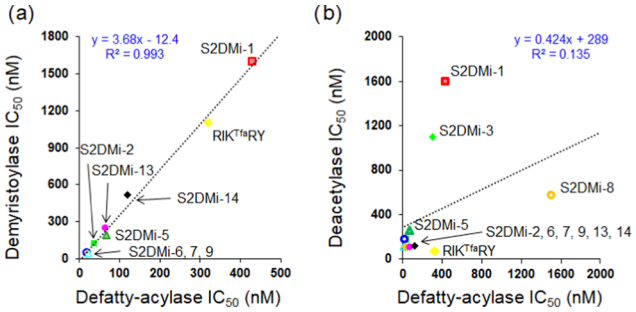

Figure 4. (a) Correlation between SIRT2 defatty-acylase-inhibitory activity evaluated by the SFP3 assay and the demyristoylase-inhibitory activity evaluated by the **p53(Myr)-AMC** assay for the indicated compounds (**RIK^{Tfa}RY**, **S2DMi-1**, **S2DMi-2**, **S2DMi-5−7**, **S2DMi-9**, **S2DMi-13**, and **S2DMi-14**). (b) Correlation between SIRT2 defatty-acylase-inhibitory activities evaluated by SFP3 and deacetylase-inhibitory activities evaluated by the FLUOR DE LYS SIRT2 assay kit for the indicated compounds (**RIK^{Tfa}RY**, **S2DMi-1−3**, **S2DMi-5−9**, **S2DMi-13**, and **S2DMi-14**). The data from Table 1 were plotted.

Three key findings of this study are as follows. First, our fluorescence probe SFP3 could measure the defatty-acylase activity of SIRT2. Therefore, it should be useful to screen small chemicals that selectively inhibit defatty-acylase activity over deacetylase activity of various sirtuins. Second, the SIRT2 recognition peptide sequence RIKRY is extremely important for potent inhibitory activity, as in **S2DMi-2**, **S2DMi-5−7**, and **S2DMi-9**. It is noteworthy that compound **TM** did not inhibit defatty-acylase activity, even though it is reported to be a potent SIRT2 inhibitor and contains a thiomyristoyl group that should be accommodated in the hydrophobic selectivity pocket. These results suggest that the combination of a suitable peptide sequence and attachment of a hydrophobic hydrocarbon, such as a thiomyristoyl group, or aromatic rings, as in Dabycl-EH, at the ε-amino group of the lysine residue is critical for SIRT2 defatty-acylase inhibition. Third, the phenylacetyl scaffold is resistant to hydrolysis by SIRT and thus should be suitable for the development of SIRT inhibitors. Modification with a thioamide moiety might be useful because most potent SIRT2 inhibitors have a thioamide moiety and bind to NAD$^+$ (mechanism-based inhibitors).[19,22] A recent study has shown that SIRT2 can deacylate benzoylated lysine, supporting our result that the Dabcyl moiety of **S2DMi-1** was cleaved by SIRT2.[30] Therefore, the phenylacetyl scaffold appears to be resistant to various SIRT2 deacylase activities, including deacetylase, demyristoylase, and debenzoylase activities.

It is noteworthy that compound **TM**, SirReal2, and AGK2 had almost no effect on SIRT2 defatty-acylase activity. Considering that **S2DMi-6** and **S2DMi-9** exhibited mixed-type inhibition, it seems likely that binding of substrates bearing a long-chain fatty acyl group, such as SFP3 and **p53(Myr)-AMC**, induces a quite dramatic conformational change of the substrate recognition pocket. As a consequence, compound **TM**, SirReal2, and AGK2 may no longer be able to bind, and therefore these inhibitors act as specific inhibitors of SIRT2's deacetylase activity.

S2DMi-6, **S2DMi-7**, and **S2DMi-9** lacked selectivity for SIRT2 over SIRT1 and 3 despite the above hypothesis that Dabcyl moieties can occupy the "SIRT2 selectivity pocket". This is because a substrate recognition pocket of SIRT2 is very flexible and the pocket structures bound with acetylated peptide and bound with myristoylated peptide are quite different to fit the shape to each substrate; in addition, the structures of the hydrophobic pockets of SIRT1−3 are reported to be all similar.[12] Therefore, this means that the

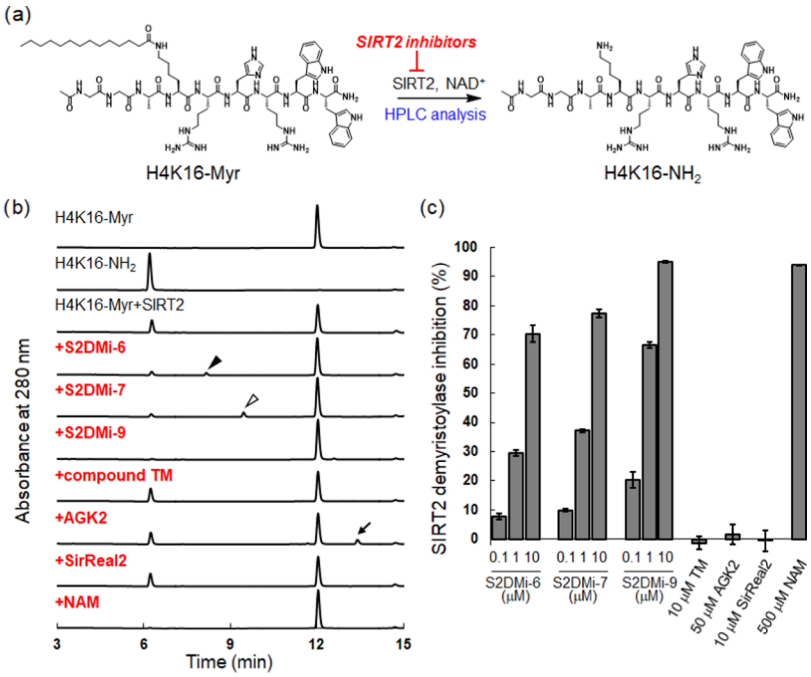

Figure 5. (a) SIRT2 inhibition assay using a peptide substrate, **H4K16-Myr**. Generation of **H4K16-NH$_2$** in the presence of SIRT2 inhibitors was monitored with HPLC. (b) HPLC analyses of the enzymatic reactions of 100 μM **H4K16-Myr**, 500 μM NAD$^+$, and 175 nM SIRT2 in the presence or absence of SIRT2 inhibitors (**S2DMi-6**, **S2DMi-7**, **S2DMi-9**, compound **TM**, SirReal2 (10 μM), AGK2 (50 μM), and NAM (500 μM)) after 2 h. Absorbance at 280 nm was monitored. A filled arrowhead, an open arrowhead, and an arrow indicate **S2DMi-6**, **S2DMi-7**, and AGK2, respectively. (c) SIRT2 inhibition (%) at the indicated concentrations of SIRT2 inhibitors. The results are mean ± S.D. (n = 3).

DOI: 10.1021/acs.jmedchem.9b00315
J. Med. Chem. XXXX, XXX, XXX−XXX

Table 2. SIRT1, 3, and 6 Inhibitory Activities (IC_{50}) and/or % Inhibition Values of RIK^{Tfa}RY, S2DMi-1−14, Compounds M, TM, AGK2, NAM, and SirReal2 Evaluated by Using SFP3 and p53(Myr)-AMC (deMyr)[e]

	SIRT1		SIRT3		SIRT6
	SFP3 (μM)	deMyr (μM)	SFP3 (μM)	deMyr (μM)	SFP3 (μM)
RIK^{Tfa}RY	>2.0, 16%[a]	32%[c]	0.54 ± 0.062	58%[c]	3.1%[a]
S2DMi-1	>2.0, 22%[a]	42%[c]	0.77 ± 0.072	34%[c]	13%[a]
S2DMi-2	0.40 ± 0.11	0.098 ± 0.009	0.11 ± 0.036	0.33 ± 0.035	40%[a]
S2DMi-3	1.7 ± 0.16	42%[c]	1.5 ± 0.12	11%[c]	13%[a]
S2DMi-4	>2.0, 8.9%[a]	3.2%[c]	>2.0, 10%[a]	−1.1%[c]	11%[a]
S2DMi-5	1.1 ± 0.30	0.14 ± 0.011	0.18 ± 0.020	0.48 ± 0.052	28%[a]
S2DMi-6	0.12 ± 0.092	0.050 ± 0.004	0.055 ± 0.007	0.19 ± 0.027	43%[a]
S2DMi-7	0.048 ± 0.006	0.071 ± 0.009	0.077 ± 0.004	0.34 ± 0.045	32%[a]
S2DMi-8	>2.0, 18%[a]	31%[c]	>2.0, 14%[a]	5.6%[c]	2.6%[a]
S2DMi-9	0.33 ± 0.018	0.026 ± 0.001	0.046 ± 0.004	0.13 ± 0.015	0.25 ± 0.069
S2DMi-10	8.8%[a]	20%[c]	5.9%[a]	2.6%[c]	3.8%[a]
S2DMi-11	1.3%[a]	2.8%[c]	−0.08%[a]	5.6%[c]	−7.4%[a]
S2DMi-12	>2.0, 2.0%[a]	6.3%[c]	>2.0, 7.0%[a]	−0.13%[c]	−0.32%[a]
S2DMi-13	0.27 ± 0.031	0.084 ± 0.008	N.D.	N.D.	28%[a]
S2DMi-14	1.4 ± 0.21	0.43 ± 0.032	N.D.	N.D.	0.64%[a]
compound **M**	−0.59%[a]	1.7%[c]	−2.3%[a]	1.7%[c]	−3.5%[a]
compound **TM**	0.81%[a]	2.7%[c]	−0.90%[a]	−1.2%[c]	−3.3%[a]
AGK2	6.8%[b]	10%[b]	27%[b]	9.1%[b]	N.D.
NAM	33 ± 1.7	N.D.	10 ± 0.72	N.D.	120 ± 13[d]
SirReal2	>10	>10	N.D.	N.D.	−2.2%[a]

[a]Inhibition (%) at 2 μM. [b]Inhibition (%) at 50 μM. [c]Inhibition (%) at 1 μM. [d]Data from ref 29. [e]The data indicate IC_{50} (mean ± S.D., n = 3) of at least two experiments. N.D. = not determined. For details, see Figures S9−S13.

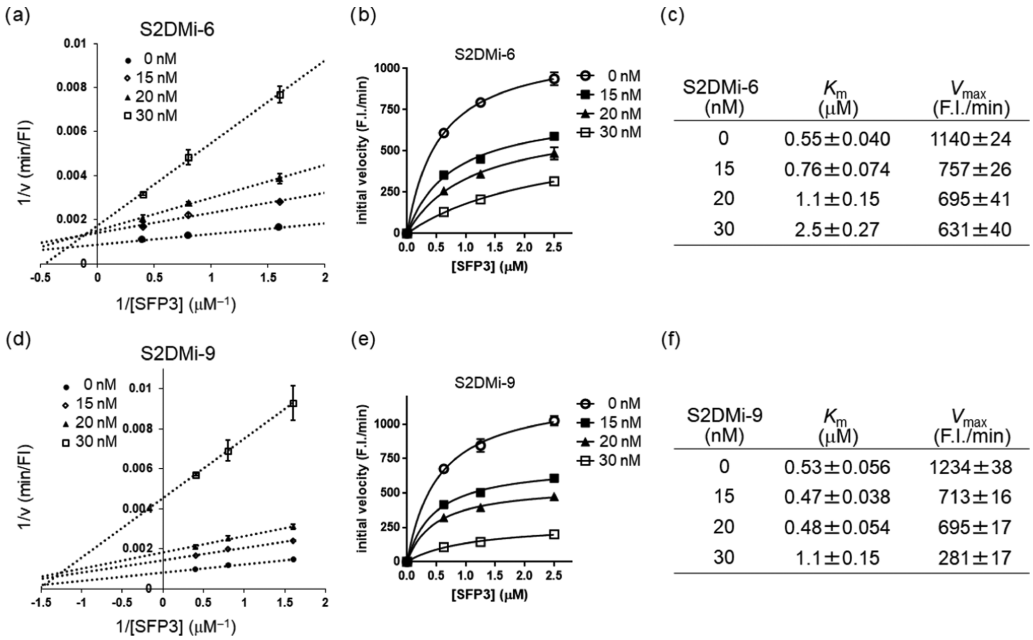

Figure 6. Competition analyses of **S2DMi-6** and **S2DMi-9** with SFP3. (a, d) Lineweaver−Burk plots of enzymatic cleavage of 0.625, 1.25, and 2.5 μM SFP3 in the presence of 35 nM SIRT2, 500 μM NAD^+, and 0, 15, 20, or 30 nM **S2DMi-6** or **S2DMi-9**. The initial velocity, v, was calculated from the changes of fluorescence intensity (F.I./min). The results are shown as mean ± S.D. (n = 3). (b, e) Michaelis−Menten plots of the data shown in (a) and (d). (c, f) K_m and V_{max} values were calculated from the data in (b) and (e).

SIRT2 selectivity pocket might be beneficial just for the development of SIRT2-selective deacetylase inhibitors, but not for SIRT2 defatty-acylase inhibitors. Given this speculation, we expect that it will be difficult to develop subtype-selective defatty-acylase inhibitors. However, selective SIRT2 defatty-acylase inhibitors are of interest because it was recently reported that SIRT2 defatty-acylase activity promotes carcinogenesis through the regulation of Ras localization.[16] Therefore, SIRT2 defatty-acylase inhibitors are candidate therapeutic agents for cancers, with a novel mechanism of action, which would be independent of SIRT2 deacetylase function, whose inhibition also has an anticancer action via c-Myc degradation.[19] The defatty-acylase activity of SIRT6 regulates TNF-α secretion and R-Ras2 localization,[9,31] so it seems likely that the defatty-acylase activities of other sirtuins also have significant biological functions distinct from those of their deacetylase

DOI: 10.1021/acs.jmedchem.9b00315
J. Med. Chem. XXXX, XXX, XXX−XXX

activities. Thus, there is a clear need for development of potent and selective inhibitors of the different activities of individual members of the SIRT family.

■ EXPERIMENTAL SECTION

General Information. Proton nuclear magnetic resonance spectra (^{1}H NMR) were recorded on a JEOL JNM-ECZ500R spectrometer in the indicated solvent. Chemical shifts (δ) are reported in parts per million relative to the internal standard, tetramethylsilane. Electrospray ionization (ESI) mass spectra (MS) were recorded on a JEOL JMS-T100LC mass spectrometer equipped with a nanospray ion source. Ultraviolet−visible-light absorption spectra were recorded on a UV-1800 spectrophotometer. Analytical HPLC was performed with a Shimadzu pump system equipped with a reversed-phase ODS column (Inertsil ODS-3 4.6 × 150 mm^2, GL Science) at a flow rate of 1.0 mL/min. Semipreparative HPLC purification was performed with a JASCO PU-2086 pump system equipped with a reversed-phase ODS column (Inertsil ODS-3 20 × 250 mm^2, GL Science) at a flow rate of 10 mL/min. Microplate fluorescence assay was performed on an ARVO X5 plate reader (PerkinElmer). Recombinant human SIRT1 was purchased from R&D Systems, SIRT2 and SIRT3 were purchased from ATGen, and SIRT6 was purchased from BioVision. The FLUOR DE LYS SIRT2 assay kit (BML-LI179-0005) was purchased from Enzo Life Sciences, Inc. Amino acids, Fmoc-NH-Sieber amide resin, Fmoc-NH-SAL resin, and 2-chlorotrityl chloride resin were purchased from Watanabe Chemical Industries, Ltd. SirReal2 was purchased from Cayman Chemical. Cell Counting Kit-8 was purchased from Dojindo. All other reagents and solvents were purchased from Sigma-Aldrich, Tokyo Chemical Industry Co., Ltd. (TCI), Wako Pure Chemical Industries, or Nacalai Tesque and used without further purification. Flash column chromatography was performed using silica gel 60 (particle size 0.032−0.075) supplied by Taiko Shoji Ltd. The purities of the synthesized compounds were assessed by HPLC, and purity was ≥95% (Figure S18). The enantiomerical purities of compounds **1**−**6** were assessed by HPLC using CHIRALPAK IA-3 (Daicel), and enantiomerical purity was ≥99% (Figure S19).

Synthesis of RIK^{Tfa}RY. RIK^{Tfa}RY was synthesized in accordance with the previous report.[28] Purity by HPLC: 98.1% (230 nm); t_R = 11.6 min (A/B = 95:5 → 90:10 (5 min) → 0:100 (20 min); A: 0.1% TFA Milli-Q, B: 0.1% TFA CH_3CN).

Syntheses of Compounds M and TM. Compounds **M** and **TM** were synthesized in accordance with the previous report.[19] Purity by HPLC: 97.6% (254 nm); t_R = 22.3 min for compound **M**, 97.5% (254 nm); t_R = 24.1 min for compound **TM** (A/B = 50:50 → 0:100 (20 min) → 0:100 (25 min); A: 0.1% TFA Milli-Q, B: 0.1% TFA CH_3CN).

Syntheses of Fmoc-Lys(Dabcyl)-OH (1), Fmoc-Lys(Dabcyl-EH)-OH (2), and Fmoc-Lys(Dabcyl-PH)-OH (3). These compounds were synthesized in accordance with our previous report.[29]

Synthesis of Fmoc-Lys(diEtDabcyl-EH)-OH (4). To a solution of Fmoc-Lys-OH·HCl (60 mg, 0.15 mmol, 1.05 equiv) and DIPEA (74 μL, 0.43 mmol, 3.0 equiv) in DMF (1 mL) was added **5** (58 mg, 0.14 mmol, 1.0 equiv). The reaction mixture was stirred at R.T. for 30 min and then AcOEt was added. The organic layer was washed with sodium phosphate buffer (pH ∼ 4) and brine, dried over Na_2SO_4, and evaporated. The residue was purified by column chromatography on silica gel (eluent: CH_2Cl_2/MeOH = 99/1 → 97/3) to afford Fmoc-Lys(diEtDabcyl-EH)-OH (**4**) (33 mg, 0.050 mmol) in 35% yield as a yellow solid. ^{1}H NMR (500 MHz, DMSO-d_6): δ 1.15 (t, 6H, J = 7.1 Hz), 1.27−1.46 (m, 4H), 1.55−1.76 (m, 2H), 3.00−3.09 (m, 2H), 3.44 (q, 4H, J = 7.1 Hz), 3.86−3.94 (m 1H), 4.18−4.24 (m, 1H), 4.25−4.31 (m, 2H), 6.77 (d, 2H, J = 9.4 Hz), 7.32 (dd, 2H, J = 7.5, 7.5 Hz), 7.37−7.44 (m, 4H), 7.62 (d, 1H, J = 8.0 Hz), 7.69 (d, 2H, J = 8.3 Hz), 7.71−7.75 (m, 4H), 7.89 (d, 2H, J = 7.5 Hz), 8.09 (t, 1H, J = 5.6 Hz); MS (ESI$^+$): 662 [M + H]$^+$.

Synthesis of Fmoc-Lys(OH-Dabcyl-EH)-OH (5). To a solution of Fmoc-Lys-OH·HCl (226 mg, 0.56 mmol, 1.2 equiv) and DIPEA (244 μL, 1.4 mmol, 3.0 equiv) in DMF (5 mL) was added **13** (185 mg, 0.47 mmol, 1.0 equiv) in DMF (1 mL). The reaction mixture was stirred at R.T. for 15 min and then AcOEt was added. The organic layer was washed with sodium phosphate buffer (pH ∼ 4) and brine, dried over Na_2SO_4, and evaporated. The residue was purified by column chromatography on silica gel (eluent: CH_2Cl_2/MeOH = 97/3 → 95/5) to afford Fmoc-Lys(OH-Dabcyl-EH)-OH (**5**) (252 mg, 0.39 mmol) in 83% yield as a yellow solid. ^{1}H NMR (500 MHz, DMSO-d_6): δ 1.28−1.46 (m, 4H), 1.54−1.76 (m, 2H), 3.00−3.09 (m, 2H), 3.42 (s, 3H), 3.49 (s, 2H), 3.85−3.96 (m 1H), 4.17−4.23 (m, 1H), 4.23−4.28 (m, 2H), 7.19 (d, 2H, J = 9.0 Hz), 7.32 (dd, 2H, J = 7.5, 7.5 Hz), 7.38−7.46 (m, 4H), 7.62 (d, 1H, J = 7.3 Hz), 7.72 (d, 2H, J = 7.5 Hz), 7.79 (d, 2H, J = 8.2 Hz), 7.86 (d, 2H, J = 8.4 Hz), 7.89 (d, 2H, J = 7.5 Hz), 8.11 (t, 1H, J = 5.5 Hz).

Synthesis of Fmoc-Lys(Dabcyl-EH-H)-OH (6). To a solution of Fmoc-Lys-OH·HCl (496 mg, 1.2 mmol, 1.2 equiv) and DIPEA (533 μL, 3.1 mmol, 3.0 equiv) in DMF (6 mL) was added a solution of **15** (344 mg, 1.0 mmol, 1.0 equiv) in DMF (2 mL). The reaction mixture was stirred at R.T. for 10 min and then AcOEt was added. The organic layer was washed with sodium phosphate buffer (pH ∼ 4) and brine, dried over Na_2SO_4, and evaporated. The residue was purified by column chromatography on silica gel (eluent: CH_2Cl_2/MeOH = 97/3 → 95/5) to afford Fmoc-Lys(Dabcyl-EH-H)-OH (**6**) (521 mg, 0.88 mmol) in 86% yield as a yellow solid. ^{1}H NMR (500 MHz, DMSO-d_6): δ 1.26−1.48 (m, 4H), 1.56−1.76 (m, 2H), 3.01−3.10 (m, 2H), 3.51 (s, 2H), 3.88−3.95 (m 1H), 4.18−4.25 (m, 1H), 4.25−4.31 (d, 2H, J = 7.0 Hz), 7.32 (dd, 2H, J = 7.4, 7.5 Hz), 7.41 (dd, 2H, J = 7.5, 7.5 Hz), 7.46 (d, 1H, J = 7.8 Hz), 7.54−7.65 (m, 4H), 7.72 (d, 2H, J = 7.5 Hz), 7.82−7.92 (m, 6H), 8.12 (t, 1H, J = 5.4 Hz).

Synthesis of 4-[(4-(Diethylamino)phenyl)diazenyl]-benzeneacetic Acid (diEtDabcyl-EH (8)). To a solution of 4-aminobenzeneacetic acid (**7**) (453 mg, 3.0 mmol, 1.0 equiv) in 1 N HCl (20 mL) was added dropwise a solution of $NaNO_2$ (310 mg, 4.5 mmol, 1.5 equiv) in H_2O (2 mL) at 0 °C. The reaction mixture was stirred at 0 °C for 30 min and then added dropwise to a solution of *N*,*N*-diethylaniline (575 μL, 3.6 mmol, 1.2 equiv) in AcOH/H_2O (10/5 mL) at 0 °C. Stirring was continued at R.T. for 2.5 h, and then 2 N NaOH was added to adjust the pH to 4. The resulting precipitate was collected by filtration and washed with cold water and Et_2O to afford diEtDabcyl-EH (**8**) (485 mg, 1.6 mmol) in 52% yield as a brown solid. MS (ESI$^+$): 312 [M + H]$^+$.

Synthesis of 2,5-Dioxopyrrolidin-1-yl 4-[(4-(diethylamino)-phenyl)diazenyl]benzeneacetate (diEtDabcyl-EH-SE (9)). To a solution of **8** (480 mg, 1.5 mmol, 1.0 equiv) and EDCI•HCl (1480 mg, 7.7 mmol, 5.0 equiv) in dry DMF (8 mL) was added *N*-hydroxysuccinimide (887 mg, 7.7 mmol, 5.0 equiv). The reaction mixture was stirred at R.T. for 3 h, and then AcOEt and sodium phosphate buffer (pH ∼ 4) were added. The organic layer was separated, washed with brine, dried over Na_2SO_4, and evaporated. The residue was purified by column chromatography on silica gel (eluent: *n*-hexane/AcOEt = 2/1 → 1/1) to afford diEtDabcyl-EH-SE (**9**) (58 mg, 0.14 mmol) in 9.2% yield as an orange solid. MS (ESI$^+$): 409 [M + H]$^+$.

Synthesis of 4-[(4-Hydroxyphenyl)diazenyl]benzeneacetic Acid (OH-Dabcyl-EH (10)). To a solution of 4-aminobenzeneacetic acid (**7**) (756 mg, 5.0 mmol, 1.0 equiv) in 2 N HCl (15 mL) and H_2O (5 mL) was added dropwise a solution of $NaNO_2$ (414 mg, 6.0 mmol, 1.2 equiv) in H_2O (1 mL) at 0 °C. The reaction mixture was stirred at 0 °C for 30 min, and then phenol (470 mg, 5.0 mmol, 1.0 equiv) in 2 N NaOH (5 mL) was added at 0 °C. The reaction mixture was stirred at 0 °C for 1.5 h. The precipitate was collected by filtration, and the residue was purified by column chromatography on silica gel (eluent: CH_2Cl_2/MeOH = 95/5) to afford OH-Dabcyl-EH (**10**) (385 mg, 1.5 mmol) in 30% yield as a yellow solid. ^{1}H NMR (500 MHz, DMSO-d_6): δ 3.67 (s, 2H), 6.94 (d, 2H, J = 8.7 Hz), 7.44 (d, 2H, J = 8.4 Hz), 7.76 (d, 2H, J = 8.4 Hz), 7.79 (d, 2H, J = 8.7 Hz), 10.31 (brs, 1H); MS (ESI$^-$): 255 [M − H]$^-$.

Synthesis of Methoxymethyl 4-[(4-(Methoxymethoxy)-phenyl)diazenyl]benzeneacetate (11). To a solution of **10** (385 mg, 1.5 mmol, 1.0 equiv) and DIPEA (1310 μL, 7.5 mmol, 5.0 equiv) in DMF (6 mL) was added dropwise MOM-Cl (342 μL, 3.0 mmol,

DOI: 10.1021/acs.jmedchem.9b00315
J. Med. Chem. XXXX, XXX, XXX−XXX

2.0 equiv) at 0 °C. The reaction mixture was stirred at 0 °C for 15 min and at R.T. for 13 h and then diluted with AcOEt, washed with sodium phosphate buffer (pH ∼ 4) and brine, dried over Na_2SO_4, and evaporated. The residue was purified by column chromatography on silica gel (eluent: *n*-hexane/AcOEt = 5/1 → 4/1) to afford **11** (445 mg, 1.3 mmol) in 86% yield as a yellow solid. ^{1}H NMR (500 MHz, DMSO-d_6): δ 3.39 (s, 3H), 3.42 (s, 3H), 3.86 (s, 2H), 5.22 (s, 2H), 5.31 (s, 2H), 7.21 (d, 2H, *J* = 8.8 Hz), 7.49 (d, 2H, *J* = 8.3 Hz), 7.83 (d, 2H, *J* = 8.3 Hz), 7.89 (d, 2H, *J* = 8.8 Hz); MS (ESI$^+$): 345 [M − H]$^+$.

Synthesis of 4-[(4-(Methoxymethoxy)phenyl)diazenyl]-benzeneacetic Acid (12). To a solution of **11** (445 mg, 1.3 mmol, 1.0 equiv) in EtOH (2 mL) was added 2 N NaOH (2 mL, 3.0 equiv). The mixture was stirred at 70 °C for 1.5 h, cooled to 0 °C, acidified with 2 N HCl, and extracted with AcOEt. The combined organic layer was washed with brine, dried over Na_2SO_4, and evaporated. The residue was purified by column chromatography on silica gel (eluent: CH_2Cl_2/MeOH = 98/2) to afford **12** (268 mg, 0.89 mmol) in 69% yield as a yellow solid. ^{1}H NMR (500 MHz, DMSO-d_6): δ 3.42 (s, 3H), 3.69 (s, 2H), 5.31 (s, 2H), 7.21 (d, 2H, *J* = 9.0 Hz), 7.46 (d, 2H, *J* = 8.3 Hz), 7.81 (d, 2H, *J* = 8.3 Hz), 7.89 (d, 2H, *J* = 9.0 Hz).

Synthesis of 2,5-Dioxopyrrolidin-1-yl 4-[(4-(methoxymethoxy)phenyl)diazenyl]benzeneacetate (13). To a solution of **12** (268 mg, 0.89 mmol, 1.0 equiv) and EDCI•HCl (855 mg, 4.5 mmol, 5.0 equiv) in dry DMF (5 mL) was added *N*-hydroxysuccinimide (513 mg, 4.5 mmol, 5.0 equiv). The reaction mixture was stirred at R.T. for 5 h, and then AcOEt and sodium phosphate buffer (pH ∼ 4) were added. The organic layer was separated, washed with brine, dried over Na_2SO_4, and evaporated. The residue was purified by column chromatography on silica gel (eluent: *n*-hexane/AcOEt = 2/1 → 1/1) to afford **13** (205 mg, 0.52 mmol) in 59% yield as an orange solid. ^{1}H NMR (500 MHz, DMSO-d_6): δ 2.82 (s, 4H), 3.42 (s, 3H), 3.85 (s, 2H), 5.31 (s, 2H), 7.22 (d, 2H, *J* = 8.8 Hz), 7.56 (d, 2H, *J* = 8.3 Hz), 7.85 (d, 2H, *J* = 8.3 Hz), 7.89 (d, 2H, *J* = 8.8 Hz).

Synthesis of 4-(2-Phenyldiazenyl)benzeneacetic Acid (Dabcyl-EH-H (14)). To a solution of nitrosobenzene (535 mg, 5.0 mmol, 1.0 equiv) in AcOH (6 mL) was added dropwise a solution of **7** (907 mg, 6.0 mmol, 1.2 equiv) in AcOH (6 mL) at R.T. The reaction mixture was stirred at R.T. for 21 h and then evaporated. The residue was purified by column chromatography on silica gel (eluent: CH_2Cl_2/MeOH = 95/5) to afford Dabcyl-EH-H (**14**) (1087 mg, 4.5 mmol) in 90% yield as a yellow solid. ^{1}H NMR (500 MHz, DMSO-d_6): δ 3.71 (s, 2H), 7.49 (d, 2H, *J* = 8.3 Hz), 7.55−7.64 (m, 3H), 7.85 (d, 2H, *J* = 8.2 Hz), 7.89 (d, 2H, *J* = 8.0 Hz).

Synthesis of 2,5-Dioxopyrrolidin-1-yl 4-4-(2-Phenyldiazenyl)benzeneacetate (Dabcyl-EH-H-SE (15)). To a solution of **14** (480 mg, 2.0 mmol, 1.0 equiv) and EDCI•HCl (1920 mg, 10 mmol, 5.0 equiv) in dry DMF (10 mL) was added *N*-hydroxysuccinimide (1150 mg, 10 mmol, 5.0 equiv). The reaction mixture was stirred at R.T. for 11 h, and then AcOEt and sodium phosphate buffer (pH ∼ 4) were added. The organic layer was separated, washed with brine, dried over Na_2SO_4, and evaporated. The residue was purified by column chromatography on silica gel (eluent: *n*-hexane/AcOEt = 2/1 → 1/1) to afford Dabcyl-EH-H-SE (**15**) (344 mg, 1.0 mmol) in 51% yield as an orange solid. ^{1}H NMR (500 MHz, DMSO-d_6): δ 2.82 (s, 4H), 4.27 (s, 2H), 7.56−7.64 (m, 5H), 7.88−7.92 (m, 4H).

Fmoc Solid-Phase Syntheses of S2DMi-1−4, S2DMi-6−8, S2DMi-13, S2DMi-14-Protected. The peptide chain was synthesized using Fmoc solid-phase chemistry on Fmoc-NH-Sieber amide resin (96 mg, 0.050 mmol) in a PD-10 Empty Column at R.T. Each assembly step was done by activating Fmoc-amino acid (0.15 mmol) with 2-(1*H*-benzotriazol-1-yl)-1,1,3,3-tetramethyluronium hexafluorophosphate (HBTU) (57 mg, 0.15 mmol), 1-hydroxybenzotriazole hydrate (HOBt·H_2O) (23 mg, 0.15 mmol), and DIPEA (53 μL, 0.30 mmol) in DMF (1.5 mL) for 1 h. The Fmoc-amino acids used in this synthesis were as follows: Fmoc-Tyr(tBu)-OH (69 mg, 0.15 mmol), Fmoc-Arg(Pbf)-OH (98 mg, 0.15 mmol), Fmoc-Lys(Dabcyl)-OH (93 mg, 0.15 mmol), Fmoc-Lys(Dabcyl-EH)-OH (94 mg, 0.15 mmol), Fmoc-Lys(Dabcyl-PH)-OH (65 mg, 0.10 mmol), Fmoc-Lys(OH-Dabcyl-EH)-OH (98 mg, 0.15 mmol), Fmoc-Lys(Dabcyl-EH-H)-OH (89 mg, 0.15 mmol), Fmoc-Val-OH (51 mg, 0.15 mmol), Fmoc-Lys(Boc)-OH (70 mg, 0.15 mmol), Fmoc-Ile-OH (53 mg, 0.15 mmol), Fmoc-Thr(tBu)-OH (60 mg, 0.15 mmol), Fmoc-Asp(tBu)-OH (62 mg, 0.15 mmol), and Fmoc-Ser(tBu)-OH (58 mg, 0.15 mmol). The Fmoc group was removed twice by using 20% piperidine in DMF (2 mL) at R.T. for 2 and 10 min. The N-terminal amino acid was acetylated with 25% Ac_2O in dichloromethane (DCM) (2 mL) for 5 min. For cleavage of the synthetic peptide without loss of side-chain-protecting groups, the resin was mixed with 1% TFA and 1% triethylsilane (TES) in DCM (2 mL) for 2 min (15 times); then, the filtrate was collected in sat. $NaHCO_3$ aq. (50 mL). The organic phase was separated, washed with brine, dried over Na_2SO_4, and evaporated to afford the following compounds.

S2DMi-1-protected (39 mg, 0.025 mmol), 49% yield as an orange solid. MS (ESI$^+$): 1609 [M + Na]$^+$.

S2DMi-2-protected (66 mg, 0.041 mmol), 82% yield as an orange solid. MS (ESI$^+$): 1601 [M + H]$^+$.

S2DMi-3-protected (68 mg, 0.042 mmol), 84% yield as an orange solid. MS (ESI$^+$): 1637 [M + Na]$^+$.

S2DMi-4-protected (33 mg, 0.032 mmol), 64% yield as an orange solid. MS (ESI$^+$): 1045 [M + Na]$^+$.

S2DMi-6-protected (34 mg, 0.041 mmol), 42% yield as a yellow solid. MS (ESI$^+$): 1640 [M + Na]$^+$.

S2DMi-7-protected (78 mg, 0.050 mmol), quantitative yield as a yellow solid. MS (ESI$^+$): 1580 [M + Na]$^+$.

S2DMi-8-protected (49 mg, 0.049 mmol), 98% yield as a yellow solid. MS (ESI$^+$): 994 [M + H]$^+$.

S2DMi-13-protected (47 mg, 0.050 mmol), quantitative yield as a yellow solid. MS (ESI$^+$): 953 [M + Na]$^+$.

S2DMi-14-protected (45 mg, 0.042 mmol), 83% yield as a yellow solid. MS (ESI$^+$): 1101 [M + Na]$^+$.

Syntheses of S2DMi-1−4, S2DMi-6−8, S2DMi-13, and S2DMi-14. To a solution of **S2DMi-1−4**, **S2DMi-6−8**, **S2DMi-13**, or **S2DMi-14-protected** in CH_2Cl_2 (3 mL) was added TFA (3 mL). The reaction mixture was stirred for 2 h at R.T. and then evaporated. The residue was purified by reversed-phase HPLC to afford the following compounds.

S2DMi-1·3TFA (22 mg, 0.0161 mmol), 65% yield as a red solid. Purity by HPLC: 96.1% (254 nm); t_R = 14.4 min (A/B = 95:5 → 90:10 (5 min) → 0:100 (20 min); A: 0.1% TFA Milli-Q, B: 0.1% TFA CH_3CN); high-resolution mass spectrometry (HRMS) (ESI$^+$): calcd: 1027.5954; found: 1027.5994 [M + H]$^+$ (+3.92 ppm).

S2DMi-2·3TFA (45 mg, 0.0325 mmol), 79% yield as a red solid. Purity by HPLC: 99.7% (254 nm); t_R = 8.6 min (A/B = 80:20 → 0:100 (20 min); A: 0.1% TFA Milli-Q, B: 0.1% TFA CH_3CN); HRMS (ESI$^+$): calcd: 1041.6110; found: 1041.6087 [M + H]$^+$ (−2.27 ppm).

S2DMi-3·3TFA (51 mg, 0.037 mmol), 87% yield as a red solid. Purity by HPLC: 99.7% (254 nm); t_R = 8.7 min (A/B = 80:20 → 0:100 (20 min); A: 0.1% TFA Milli-Q, B: 0.1% TFA CH_3CN); HRMS (ESI$^+$): calcd: 1055.6267; found: 1055.6257 [M + H]$^+$ (−0.93 ppm).

S2DMi-4·TFA (13 mg, 0.0134 mmol), 42% yield as a red solid. Purity by HPLC: 95.9% (254 nm); t_R = 14.8 min (A/B = 95:5 → 90:10 (5 min) → 0:100 (20 min); A: 0.1% TFA Milli-Q, B: 0.1% TFA CH_3CN); HRMS (ESI$^+$): calcd: 877.4184; found: 877.4192 [M + Na]$^+$ (+0.92 ppm).

S2DMi-6·2TFA (11 mg, 0.0089 mmol), 22% yield as a yellow solid. Purity by HPLC: 98.7% (254 nm); t_R = 10.2 min (A/B = 80:20 → 0:100 (20 min); A: 0.1% TFA Milli-Q, B: 0.1% TFA CH_3CN); HRMS (ESI$^+$): calcd: 1014.5637; found: 1014.5682 [M + H]$^+$ (+4.37 ppm).

S2DMi-7·2TFA (37 mg, 0.030 mmol), 60% yield as a yellow solid. Purity by HPLC: 97.7% (254 nm); t_R = 10.1, 11.4 min (A/B = 80:20 → 0:100 (20 min); A: 0.1% TFA Milli-Q, B: 0.1% TFA CH_3CN); HRMS (ESI$^+$): calcd: 998.5688; found: 998.5670 [M + H]$^+$ (−1.87 ppm).

DOI: 10.1021/acs.jmedchem.9b00315
J. Med. Chem. XXXX, XXX, XXX−XXX

S2DMi-8 (16 mg, 0.019 mmol), 39% yield as a yellow solid. Purity by HPLC: 98.2% (254 nm); t_R = 8.7, 10.5 min (A/B = 80:20 → 0:100 (20 min); A: 0.1% TFA Milli-Q, B: 0.1% TFA CH_3CN); HRMS (ESI^+): calcd: 848.3919; found: 848.3908 $[M + Na]^+$ (−1.28 ppm).

S2DMi-13·TFA (23 mg, 0.029 mmol), 58% yield as a yellow solid. Purity by HPLC: 98.2% (254 nm); t_R = 8.8, 10.6 min (A/B = 80:20 → 0:100 (20 min); A: 0.1% TFA Milli-Q, B: 0.1% TFA CH_3CN); HRMS (ESI^+): calcd: 679.4044; found: 679.4049 $[M + Na]^+$ (+0.71 ppm).

S2DMi-14·2TFA (14 mg, 0.013 mmol), 30% yield as a yellow solid. Purity by HPLC: 98.8% (254 nm); t_R = 7.3, 8.8 min (A/B = 80:20 → 0:100 (20 min); A: 0.1% TFA Milli-Q, B: 0.1% TFA CH_3CN); HRMS (ESI^+): calcd: 878.5616; found: 878.5630 $[M + H]^+$ (+1.53 ppm).

Fmoc Solid-Phase Synthesis of S2DMi-5. The peptide chain was synthesized using Fmoc solid-phase chemistry on Fmoc-NH-SAL resin (72 mg, 0.050 mmol) in a PD-10 Empty Column at R.T. Each assembly step was done by activating Fmoc-amino acid (0.15 mmol) with HBTU (57 mg, 0.15 mmol), HOBt·H_2O (23 mg, 0.15 mmol), and DIPEA (53 μL, 0.30 mmol) in DMF (1.5 mL) for 1 h. The Fmoc-amino acids used in this synthesis were as follows: Fmoc-Tyr(tBu)-OH (69 mg, 0.15 mmol), Fmoc-Arg(Pbf)-OH (98 mg, 0.15 mmol), Fmoc-Lys(diEtDabcyl-EH)-OH (33 mg, 0.05 mmol), and Fmoc-Ile-OH (53 mg, 0.15 mmol). The Fmoc group was removed twice by using 20% piperidine in DMF (2 mL) at R.T. for 2 and 10 min. The reaction mixture after the condensation with Fmoc-Lys(diEtDabcyl-EH)-OH and N-terminal amino acid was treated with 25% Ac_2O in DCM (2 mL) for 5 min. For cleavage of the synthetic peptide, the resin was gently stirred in TFA/H_2O/TES (1800/100/100 μL) for 90 min, and then the filtrate was collected and evaporated to afford crude **S2DMi-5** (60 mg). The crude product was purified by reversed-phase HPLC to afford **S2DMi-5·3TFA** (8.0 mg, 0.0057 mmol) in 11% yield as a red solid. Purity by HPLC: 95.8% (254 nm); t_R = 8.2 min (A/B = 80:20 → 0:100 (20 min); A: 0.1% TFA Milli-Q, B: 0.1% TFA CH_3CN); HRMS (ESI^+): calcd: 1069.6423; found: 1069.6418 $[M + H]^+$ (−0.46 ppm).

Synthesis of Fmoc-Lys(Myr)-OH (17). To a solution of Fmoc-Lys-OH·HCl (**16**) (609 mg, 1.4 mmol, 1.0 equiv) and Na_2CO_3 (458 mg, 4.3 mmol, 3.0 equiv) in H_2O/dioxane (10 mL/8 mL) was added dropwise a solution of myristoyl chloride (466 μL, 1.7 mmol, 1.2 equiv) in dioxane (8 mL) at 0 °C. The reaction mixture was stirred under N_2 for 3 h at R.T. and then diluted with CH_2Cl_2. The organic phase was washed with 1 N HCl and brine, dried over Na_2SO_4, and evaporated. The residue was purified by column chromatography on silica gel (eluent: CH_2Cl_2/MeOH = 3/97 → 10/90) to afford **Fmoc-Lys(Myr)-OH (17)** (653 mg, 1.1 mmol) in 78% yield as a white solid. ^1H NMR (500 MHz, DMSO-d_6): δ 0.84 (t, 3H, *J* = 7.0 Hz), 1.16−1.74 (m, 28H), 2.02 (t, 2H, *J* = 7.4 Hz), 2.95−3.06 (m, 2H), 3.86−3.94 (m, 1H), 4.18−4.31 (m, 3H), 7.33 (dd, 2H, *J* = 7.3, 7.4 Hz), 7.42 (dd, 2H, *J* = 7.4, 7.4 Hz), 7.60 (d, 1H, *J* = 8.0 Hz), 7.70−7.79 (m, 3H), 7.89 (d, 2H, *J* = 7.5 Hz).

Synthesis of Fmoc-Lys(thioMyr)-OH (18). To a solution of **Fmoc-Lys(Myr)-OH (17)** (139 mg, 0.24 mmol, 1.0 equiv) in THF (5 mL) was added Lawesson's reagent (97 mg, 0.24 mmol, 1.0 equiv). The reaction mixture was stirred at R.T. for 2 h under N_2 and then evaporated. The residue was purified by column chromatography on silica gel (eluent: CH_2Cl_2/MeOH = 3/97 → 5/95) to afford **Fmoc-Lys(thioMyr)-OH (18)** (98 mg, 0.17 mmol) in 69% yield as a white solid. ^1H NMR (500 MHz, DMSO-d_6): δ 0.88 (t, 3H, *J* = 8.0 Hz), 1.19−2.02 (m, 28H), 2.59 (t, 2H, *J* = 7.5 Hz), 3.60−3.71 (m, 2H), 3.86−3.94 (m, 1H), 4.23 (t, 1H, *J* = 6.8 Hz), 4.35−4.61 (m, 3H), 5.38 (d, 1H, *J* = 7.0 Hz), 7.32 (dd, 2H, *J* = 7.4, 7.5 Hz), 7.37−7.44 (m, 3H), 7.55−7.63 (m, 2H), 7.77 (d, 2H, *J* = 7.5 Hz); (ESI^+): 594 $[M + H]^+$.

Fmoc Solid-Phase Synthesis of S2DMi-9-Protected. The peptide chain was synthesized using Fmoc solid-phase chemistry on Fmoc-NH-Sieber amide resin (96 mg, 0.050 mmol) in a PD-10 Empty Column at R.T. Each assembly step was done by activating Fmoc-amino acid (0.15 mmol) with HBTU (57 mg, 0.15 mmol), HOBt·H_2O (23 mg, 0.15 mmol), and DIPEA (53 μL, 0.30 mmol) in DMF (1.5 mL) for 1 h. The Fmoc-amino acids used in this synthesis were as follows: Fmoc-Tyr(tBu)-OH (69 mg, 0.15 mmol), Fmoc-Arg(Pbf)-OH (98 mg, 0.15 mmol), Fmoc-Lys(thioMyr)-OH (98 mg, 0.17 mmol), and Fmoc-Ile-OH (53 mg, 0.15 mmol). The Fmoc group was removed twice by using 20% piperidine in DMF (2 mL) at R.T. for 2 and 10 min. The *N*-terminal amino acid was acetylated with 25% Ac_2O in DCM (2 mL) for 5 min. For cleavage of the synthetic peptide without loss of side-chain-protecting groups, the resin was mixed with 1% TFA and 1% TES in DCM (2 mL) for 2 min (15 times), and the filtrate was collected in sat. $NaHCO_3$ aq. (50 mL). The organic phase was separated, washed with brine, dried over Na_2SO_4, and evaporated to afford **S2DMi-9-protected** (77 mg, 0.049 mmol) in 99% yield as a white solid. MS (ESI^+): 1563 $[M + H]^+$.

Synthesis of S2DMi-9. To a solution of **S2DMi-9-protected** (37 mg, 0.0237 mmol) in CH_2Cl_2 (3 mL) was added TFA (3 mL). The reaction mixture was stirred for 2 h at R.T. and then evaporated. The residue was purified by reversed-phase HPLC to afford **S2DMi-9·2TFA** (10 mg, 0.0083 mmol) in 35% yield as a white solid. Purity by HPLC: 98.8% (254 nm); t_R = 11.9 min (A/B = 70:30 → 0:100 (20 min); A: 0.1% TFA Milli-Q, B: 0.1% TFA CH_3CN); HRMS (ESI^+): calcd: 1002.6650; found: 1002.6639 $[M + H]^+$ (−1.14 ppm).

Synthesis of Cbz-Lys(OH-Dabcyl-EH)-OH (20). To a solution of Cbz-Lys-OH (**19**) (320 mg, 1.1 mmol, 1.1 equiv) and DIPEA (543 μL, 3.1 mmol, 3.0 equiv) in DMF (8 mL) was added **13** (413 mg, 1.0 mmol, 1.0 equiv). The reaction mixture was stirred at R.T. for 2.5 h, and then AcOEt was added. The organic layer was washed with sodium phosphate buffer (pH ∼ 4) and brine, dried over Na_2SO_4, and evaporated. The residue was purified by column chromatography on silica gel (eluent: CH_2Cl_2/MeOH = 96/4) to afford **Cbz-Lys(OH-Dabcyl-EH)-OH (20)** (435 mg, 0.77 mmol) in 74% yield as a yellow solid. ^1H NMR (500 MHz, DMSO-d_6): δ 1.28−1.45 (m, 4H), 1.53−1.74 (m, 2H), 3.01−3.08 (m, 2H), 3.42 (s, 3H), 3.49 (s, 2H), 3.85−3.95 (m 1H), 5.00−5.06 (m, 2H), 5.30 (s, 2H), 7.20 (d, 2H, *J* = 9.0 Hz), 7.25−7.39 (m, 5H), 7.43 (d, 2H, *J* = 8.2 Hz), 7.53 (d, 1H, *J* = 8.0 Hz), 7.78 (d, 2H, *J* = 8.2 Hz), 7.87 (d, 2H, *J* = 8.0 Hz), 8.09 (t, 1H, *J* = 5.4 Hz).

Synthesis of Cbz-Lys(OH-Dabcyl-EH)-Ala-NH_2 (21). To a solution of **Cbz-Lys(OH-Dabcyl-EH)-OH (20)** (432 mg, 0.77 mmol, 1.0 equiv), COMU (395 mg, 0.92 mmol, 1.2 equiv), and DIPEA (402 μL, 2.3 mmol, 3.0 equiv) in DMF (6 mL) was added H-Ala-NH_2·HCl (115 mg, 0.92 mmol, 1.2 equiv). The reaction mixture was stirred at R.T. for 12 h, and then AcOEt was added. The precipitate was collected to afford **Cbz-Lys(OH-Dabcyl-EH)-Ala-NH_2 (21)** (409 mg, 0.64 mmol) in 84% yield as a yellow solid. ^1H NMR (500 MHz, DMSO-d_6): δ 1.20 (d, 3H, *J* = 7.0 Hz), 1.23−1.70 (m, 6H), 2.98−3.09 (m, 2H), 3.42 (s, 3H), 3.50 (s, 2H), 3.92−3.99 (m 1H), 4.16−4.23 (m, 1H), 5.02 (s, 2H), 5.30 (s, 2H), 7.00 (brs, 1H), 7.21 (d, 2H, *J* = 9.0 Hz), 7.26−7.38 (m, 6H), 7.40−7.46 (m, 3H), 7.78 (d, 2H, *J* = 8.3 Hz), 7.88 (d, 2H, *J* = 7.9 Hz), 8.09 (t, 1H, *J* = 5.5 Hz).

Synthesis of S2DMi-10. To a solution of **Cbz-Lys(OH-Dabcyl-EH)-Ala-NH_2 (21)** (409 mg, 0.64 mmol) in CH_2Cl_2 (9 mL) was added TFA (9 mL). The reaction mixture was stirred at R.T. for 1 h and then evaporated. The residue was purified by column chromatography on silica gel (eluent: CH_2Cl_2/MeOH = 97/3 → 92/8) to afford **S2DMi-10** (289 mg, 0.49 mmol) in 76% yield as an orange solid. ^1H NMR (500 MHz, DMSO-d_6): δ 1.20 (d, 3H, *J* = 7.1 Hz), 1.24−1.70 (m, 6H), 2.98−3.08 (m, 2H), 3.48 (s, 2H), 3.92−3.99 (m 1H), 4.16−4.24 (m, 1H), 5.02 (s, 2H), 6.93 (d, 2H, *J* = 8.7 Hz), 7.00 (brs, 1H), 7.26−7.38 (m, 6H), 7.39−7.43 (m, 3H), 7.74 (d, 2H, *J* = 8.3 Hz), 7.78 (d, 2H, *J* = 9.7 Hz), 8.07 (t, 1H, *J* = 5.5 Hz), 10.26 (s, 1H); purity by HPLC: 95.4% (254 nm); t_R = 13.6 min (A/B = 80:20 → 0:100 (20 min); A: 0.1% TFA Milli-Q, B: 0.1% TFA CH_3CN); HRMS (ESI^+): calcd: 589.2775; found: 589.2779 $[M + H]^+$ (+0.72 ppm).

Synthesis of S2DMi-11. To a solution of **S2DMi-10** (59 mg, 0.10 mmol, 1.0 equiv), Cs_2CO_3 (39 mg, 0.12 mmol, 1.2 equiv), and TBAI (3.7 mg, 0.010 mmol, 0.10 equiv) in DMF (2 mL) was added benzyl bromide (18 μL, 0.15 mmol, 1.5 equiv). The reaction mixture was stirred at R.T. for 2 h and then AcOEt was added. The organic layer

DOI: 10.1021/acs.jmedchem.9b00315
J. Med. Chem. XXXX, XXX, XXX−XXX

was washed with sodium phosphate buffer (pH ∼ 4) and brine, dried over Na_2SO_4, and evaporated. The residue was purified by column chromatography on silica gel (eluent: CH_2Cl_2/MeOH = 97/3 → 93/7) to afford **S2DMi-11** (57 mg, 0.084 mmol) in 84% yield as a light-yellow solid. ^{1}H NMR (500 MHz, DMSO-d_6): δ 1.20 (d, 3H, *J* = 7.0 Hz), 1.22−1.69 (m, 6H), 2.96−3.08 (m, 2H), 3.49 (s, 2H), 3.92−3.99 (m 1H), 4.16−4.24 (m, 1H), 5.02 (s, 2H), 5.23 (s, 2H), 7.00 (brs, 1H), 7.21 (d, 2H, *J* = 9.0 Hz), 7.25−7.46 (m, 12H), 7.49 (d, 2H, *J* = 7.3 Hz), 7.78 (d, 2H, *J* = 8.4 Hz), 7.84−7.91 (m, 3H), 8.08 (t, 1H, *J* = 5.5 Hz); purity by HPLC: 95.9% (254 nm); t_R = 16.0, 18.3 min (A/B = 80:20 → 0:100 (20 min); A: 0.1% TFA Milli-Q, B: 0.1% TFA CH_3CN); HRMS (ESI$^+$): calcd: 701.3064; found: 701.3049 [M + Na]$^+$ (−2.01 ppm).

Synthesis of S2DMi-12. To a solution of **S2DMi-10** (59 mg, 0.10 mmol, 1.0 equiv), Cs_2CO_3 (49 mg, 0.15 mmol, 1.5 equiv), and TBAI (3.7 mg, 0.010 mmol, 0.10 equiv) in DMF (2 mL) was added phenethyl bromide (41 μL, 0.30 mmol, 3.0 equiv). The reaction mixture was stirred at R.T. for 48 h, and then AcOEt was added. The organic layer was washed with sodium phosphate buffer (pH ∼ 4) and brine, dried over Na_2SO_4, and evaporated. The residue was purified by column chromatography on silica gel (eluent: CH_2Cl_2/MeOH = 97/3 → 94/6) to afford **S2DMi-12** (29 mg, 0.042 mmol) in 42% yield as a light-yellow solid. ^{1}H NMR (500 MHz, DMSO-d_6): δ 1.20 (d, 3H, *J* = 7.0 Hz), 1.22−1.44 (m, 4H), 1.45−1.56 (m, 1H), 1.58−1.68 (m, 1H), 2.97−3.06 (m, 2H), 3.08 (t, 2H, *J* = 6.8 Hz), 3.49 (s, 2H), 3.92−3.99 (m 1H), 4.16−4.24 (m, 1H), 4.31 (t, 2H, *J* = 6.8 Hz), 5.02 (s, 2H), 7.00 (brs, 1H), 7.13 (d, 2H, *J* = 9.0 Hz), 7.22−7.26 (m, 1H), 7.27−7.38 (m, 10H), 7.40−7.45 (m, 3H), 7.77 (d, 2H, *J* = 8.3 Hz), 7.83−7.90 (m, 3H), 8.08 (t, 1H, *J* = 5.8 Hz); purity by HPLC: 97.6% (254 nm); t_R = 13.7, 16.6 min (A/B = 70:30 → 0:100 (20 min); A: 0.1% TFA Milli-Q, B: 0.1% TFA CH_3CN); HRMS (ESI$^+$): calcd: 693.3401; found: 693.3389 [M + H]$^+$ (−1.65 ppm).

Synthesis of 23. To a solution of Cbz-Lys(Boc)-OH (495 mg, 1.1 mmol, 1.0 equiv), COMU (758 mg, 1.8 mmol, 1.5 equiv), and DIPEA (617 μL, 3.5 mmol, 3.0 equiv) in DMF (6 mL) was added 7-amino-4-methylcoumarin (**22**) (207 mg, 1.2 mmol, 1.1 equiv) at R.T. The reaction mixture was stirred at R.T. for 8 h and then extracted with AcOEt. The organic layer was washed with sodium phosphate buffer (pH ∼ 4), 0.1 N HCl, and brine, dried over Na_2SO_4, and evaporated. The residue was purified by column chromatography on silica gel (eluent: *n*-hexane/AcOEt = 3/2 → 1/1) to afford **23** (240 mg, 0.45 mmol) in 38% yield as a white solid. ^{1}H NMR (500 MHz, DMSO-d_6): δ 1.20−1.42 (m, 13H), 1.58−1.72 (m, 2H), 2.40 (s, 3H), 2.85−2.92 (m, 2H), 4.08−4.16 (m 1H), 5.03 (s, 2H), 6.27 (s, 1H), 6.76 (t, 1H, *J* = 5.0 Hz), 7.29−7.40 (m, 5H), 7.50 (dd, 1H, *J* = 1.6, 8.6 Hz), 7.63 (d, 1H, *J* = 6.0 Hz), 7.73 (d, 1H, *J* = 8.6 Hz), 7.77 (d, 1H, *J* = 1.6 Hz), 10.47 (s, 1H).

Synthesis of 24. To a solution of **23** (238 mg, 0.44 mmol) in CH_2Cl_2 (6 mL) was added TFA (6 mL) at R.T. The reaction mixture was stirred at R.T. for 1 h and then evaporated. The residue was dissolved in AcOEt and the solution was basified with 1 N NaOH. The organic phase was washed with brine, dried over Na_2SO_4, and evaporated to afford **24** (150 mg, 0.34 mmol) in 77% yield as a white solid. ^{1}H NMR (500 MHz, DMSO-d_6): δ 1.26−1.46 (m, 4H), 1.58−1.73 (m, 2H), 2.41 (s, 3H), 4.10−4.18 (m 1H), 5.04 (s, 2H), 6.27 (s, 1H), 7.15−7.42 (m, 6H), 7.51 (dd, 1H, *J* = 1.6, 8.7 Hz), 7.67 (d, 1H, *J* = 7.7 Hz), 7.73 (d, 1H, *J* = 8.7 Hz), 7.78 (d, 1H, *J* = 1.6 Hz); MS (ESI$^+$): 438 [M + H]$^+$.

Synthesis of 25. To a solution of **24** (76 mg, 0.17 mmol, 1.0 equiv) and DIPEA (76 μL, 0.44 mmol, 2.5 equiv) in CH_2Cl_2 (10 mL) was added myristoyl chloride (56 μL.0.21 mmol, 1.2 equiv) at R.T. The reaction mixture was stirred at R.T. for 30 min and then evaporated. The residue was purified by column chromatography on silica gel (eluent: *n*-hexane/AcOEt = 1/1 → AcOEt) to afford **25** (85 mg, 0.13 mmol) in 75% yield as a white solid. ^{1}H NMR (500 MHz, $CDCl_3$): δ 0.86 (t, 3H, *J* = 6.7 Hz), 1.18−1.31 (m, 22H), 1.38−1.50 (m, 2H), 1.56−1.64 (m, 3H), 1.68−1.80 (m, 1H), 2.16 (t, 2H, *J* = 7.5 Hz), 2.41 (s, 3H), 3.18−3.40 (m, 2H), 4.24−4.32 (m, 1H), 5.12 (s, 2H), 5.58−5.70 (m, 2H), 6.19 (s, 1H), 7.28−7.38 (m, 5H), 7.48−7.55 (m, 2H), 7.66 (brs, 1H), 9.06 (brs, 1H).

Synthesis of 26. To a solution of **25** (85 mg, 0.13 mmol) in MeOH/CH_2Cl_2 (8 mL/7 mL) was added Pd/C. The reaction mixture was stirred at R.T. under H_2 for 1.5 h and then filtered through Celite. The filtrate was evaporated to afford **26** (69 mg, 0.13 mmol) in quantitative yield as a white solid. ^{1}H NMR (500 MHz, DMSO-d_6): δ 0.85 (t, 3H, *J* = 6.8 Hz), 1.16−1.51 (m, 27H), 1.60−1.70 (m, 1H), 1.99 (t, 2H, *J* = 7.5 Hz), 2.40 (s, 3H), 2.95−3.05 (m, 2H), 6.26 (s, 1H),7.56 (dd, 1H, *J* = 2.1, 8.6 Hz), 7.68−7.74 (m, 2H), 7.84 (d, 1H, *J* = 2.1 Hz); MS (ESI$^+$): 514 [M + H]$^+$.

Synthesis of 27. To a solution of **Ac-R(Pbf)H(Trt)K(Boc)-OH** (**29**) (50 mg, 0.047 mmol, 1.0 equiv), COMU (30 mg, 0.070 mmol, 1.5 equiv), and DIPEA (16 μL, 0.093 mmol, 2.0 equiv) in DMF (2 mL) was added **26** (29 mg, 0.056 mmol, 1.2 equiv). The reaction mixture was stirred at R.T. for 1 h and then AcOEt was added. The organic layer was washed with sodium phosphate buffer (pH ∼ 4), sat. $NaHCO_3$, and brine, dried over Na_2SO_4, and evaporated. The residue was purified by column chromatography on silica gel (eluent: CH_2Cl_2/MeOH = 3/97 → 8/92) to afford **27** (51 mg, 0.032 mmol) in 70% yield as a white solid. MS (ESI$^+$): 1571 [M + H]$^+$.

Synthesis of Ac-R(Pbf)H(Trt)K(Boc)-OH (29). Attachment of the first amino acid to 2-chlorotrityl chloride resin (63 mg, 0.10 mmol) was performed by reacting Fmoc-Lys(Boc)-OH (70 mg, 0.15 mmol) and DIPEA (87 μL, 0.50 mmol) with the resin in CH_2Cl_2 (2 mL) for 2 h using a PD-10 Empty Column. The peptide chain was synthesized using Fmoc solid-phase chemistry at R.T. Each assembly step was done by activating Fmoc-His(Trt)-OH (186 mg, 0.30 mmol) or Fmoc-Arg(Pbf)-OH (195 mg, 0.30 mmol) with HBTU (113 mg, 0.30 mmol), HOBt·H_2O (46 mg, 0.30 mmol), and DIPEA (105 μL, 0.60 mmol) in DMF (2 mL) for 1 h. The Fmoc group was removed with 20% piperidine in DMF (2 mL) at R.T. twice, for 2 min and 10 min. The *N*-terminal amino acid was acetylated with 25% Ac_2O in CH_2Cl_2 (2 mL) for 5 min. For cleavage of the synthetic peptide without loss of side-chain-protecting groups, the resin was mixed with 1% TFA in CH_2Cl_2 (2 mL) for 1 min (6 times, monitored with TLC), and then the filtrate was collected in 10% pyridine in MeOH (2 mL), after which the solution was evaporated. The residue was dissolved in AcOEt. This solution was washed with 0.1 N HCl and brine, dried over Na_2SO_4, and evaporated to afford **Ac-R(Pbf)H(Trt)K(Boc)-OH** (**29**) (94 mg, 0.087 mmol) in 87% yield as a white solid. MS (ESI$^+$): 1076 [M + H]$^+$.

Synthesis of p53(Myr)-AMC. To a solution of **27** (51 mg, 0.032 mmol) in CH_2Cl_2 (5 mL) was added TFA (7 mL). The reaction mixture was stirred at R.T. for 2.5 h and then evaporated. The residue was purified by reversed-phase HPLC to afford **p53(Myr)-AMC** (25 mg, 0.019 mmol) in 58% yield as a white solid. ^{1}H NMR (500 MHz, DMSO-d_6): δ 0.84 (t, 3H, *J* = 6.8 Hz), 1.12−1.78 (m, 38H), 1.87 (s, 3H), 2.00 (t, 2H, *J* = 7.5 Hz), 2.41 (s, 3H), 2.70−2.81 (m, 2H), 2.93−3.20 (m, 6H), 4.10−4.18 (m, 1H), 4.22−4.31 (m, 1H), 4.31−4.39 (m, 1H), 4.54−4.64 (m, 1H), 6.30 (s, 1H), 7.36 (s, 1H), 7.44 (d 1H, *J* = 8.8 Hz), 7.58−7.63 (m, 1H), 7.68−7.78 (m, 4H), 7.80−7.87 (m, 2H), 8.08 (d, 1H, *J* = 6.8 Hz), 8.18 (d, 1H, *J* = 7.0 Hz), 8.26 (d, 1H, *J* = 7.8 Hz), 8.37 (d, 1H, *J* = 6.7 Hz), 8.90 (s, 1H); purity by HPLC: 97.2% (254 nm); t_R = 9.97 min (A/B = 70: 30 → 0: 100 (20 min), A: 0.1% TFA Milli-Q, B: 0.1% TFA CH_3CN,); HRMS (ESI$^+$): calcd: 977.6300; found: 977.6318 [M + H]$^+$ (+1.82 ppm).

Synthesis of H4K16-NH_2-Protected. The peptide chain was synthesized using Fmoc solid-phase chemistry on Fmoc-NH-Sieber amide resin (49 mg, 0.025 mmol) in a PD-10 Empty Column at R.T. Each assembly step was done by activating Fmoc-amino acid (0.075 mmol) with HBTU (29 mg, 0.075 mmol), HOBt·H_2O (12 mg, 0.075 mmol), and DIPEA (27 μL, 0.15 mmol) in DMF (1.0 mL) for 1 h. The Fmoc-amino acids used in this synthesis were as follows: Fmoc-Trp(Boc)-OH (40 mg, 0.075 mmol), Fmoc-Arg(Pbf)-OH (49 mg, 0.075 mmol), Fmoc-His(Trt)-OH (47 mg, 0.075 mmol), Fmoc-Lys(boc)-OH (35 mg, 0.075 mmol), Fmoc-Ala-OH (25 mg, 0.075 mmol), and Fmoc-Gly-OH (22 mg, 0.075 mmol). The Fmoc group was removed twice by using 20% piperidine in DMF (2 mL) at R.T. for 2 and 10 min. The *N*-terminal amino acid was acetylated with 25% Ac_2O in DCM (2 mL) for 5 min. For cleavage of the synthetic peptide without loss of side-chain-protecting groups, the resin was mixed with

DOI: 10.1021/acs.jmedchem.9b00315
J. Med. Chem. XXXX, XXX, XXX−XXX

1% TFA and 1% TES in DCM (2 mL) for 2 min (15 times), and the filtrate was collected in sat. $NaHCO_3$ aq. (50 mL). The organic phase was separated, washed with brine, dried over Na_2SO_4, and then evaporated to afford **H4K16-NH$_2$-protected** (58 mg, 0.026 mmol) in quantitative yield as a white solid. MS (ESI$^+$): 2263.9 [M + Na]$^+$.

Synthesis of H4K16-Ac-Protected. The peptide chain was synthesized using Fmoc solid-phase chemistry on Fmoc-NH-Sieber amide resin (98 mg, 0.050 mmol) in a PD-10 Empty Column at R.T. Each assembly step was done by activating Fmoc-amino acid (0.15 mmol) with HBTU (57 mg, 0.15 mmol), HOBt·H_2O (23 mg, 0.15 mmol), and DIPEA (53 μL, 0.30 mmol) in DMF (1.5 mL) for 1 h. The Fmoc-amino acids used in this synthesis were as follows: Fmoc-Trp(Boc)-OH (79 mg, 0.15 mmol), Fmoc-Arg(Pbf)-OH (98 mg, 0.15 mmol), Fmoc-His(Trt)-OH (93 mg, 0.15 mmol), Fmoc-Lys(Ac)-OH (63 mg, 0.15 mmol), Fmoc-Ala-OH (50 mg, 0.15 mmol), and Fmoc-Gly-OH (44 mg, 0.15 mmol). The Fmoc group was removed twice by using 20% piperidine in DMF (2 mL) at R.T. for 2 and 10 min. The *N*-terminal amino acid was acetylated with 25% Ac_2O in DCM (2 mL) for 5 min. For cleavage of the synthetic peptide without loss of side-chain-protecting groups, the resin was mixed with 1% TFA and 1% TES in DCM (2 mL) for 2 min (15 times), and the filtrate was collected in sat. $NaHCO_3$ aq. (50 mL). The organic phase was separated, washed with brine, dried over Na_2SO_4, and then evaporated to afford **H4K16-Ac-protected** (107 mg, 0.049 mmol) in 98% yield as a white solid.

Synthesis of H4K16-Myr-Protected. The peptide chain was synthesized using Fmoc solid-phase chemistry on Fmoc-NH-Sieber amide resin (49 mg, 0.025 mmol) in a PD-10 Empty Column at R.T. Each assembly step was done by activating Fmoc-amino acid (0.075 mmol) with HBTU (29 mg, 0.075 mmol), HOBt·H_2O (12 mg, 0.075 mmol), and DIPEA (27 μL, 0.15 mmol) in DMF (1.0 mL) for 1 h. The Fmoc-amino acids used in this synthesis were as follows: Fmoc-Trp(Boc)-OH (40 mg, 0.075 mmol), Fmoc-Arg(Pbf)-OH (49 mg, 0.075 mmol), Fmoc-His(Trt)-OH (47 mg, 0.075 mmol) **Fmoc-Lys(Myr)-OH** (44 mg, 0.075 mmol), Fmoc-Ala-OH (25 mg, 0.075 mmol), and Fmoc-Gly-OH (22 mg, 0.075 mmol). The Fmoc group was removed twice by using 20% piperidine in DMF (2 mL) at R.T. for 2 and 10 min. The *N*-terminal amino acid was acetylated with 25% Ac_2O in DCM (2 mL) for 5 min. For cleavage of the synthetic peptide without loss of side-chain-protecting groups, the resin was mixed with 1% TFA and 1% TES in DCM (2 mL) for 2 min (15 times), and the filtrate was collected in sat. $NaHCO_3$ aq. (50 mL). The organic phase was separated, washed with brine, dried over Na_2SO_4, and then evaporated to afford **H4K16-Myr-protected** (56 mg, 0.024 mmol) in 95% yield as a white solid. MS (ESI$^+$): 2352 [M + H]$^+$.

Synthesis of H4K16-NH$_2$. To a solution of **H4K16-NH$_2$-protected** (58 mg, 0.026 mmol) in CH_2Cl_2 (3 mL) was added TFA (3 mL). The reaction mixture was stirred for 3 h at R.T. and then evaporated. The residue was purified by reversed-phase HPLC to afford **H4K16-NH$_2$·4TFA** (25 mg, 0.015 mmol) in 61% yield as a white solid. Purity by HPLC: 98.4% (254 nm); t_R = 6.17 min (A/B = 80:20 → 0:100 (20 min); A: 0.1% TFA Milli-Q, B: 0.1% TFA CH_3CN); HRMS (ESI$^+$): calcd: 1195.6475; found: 1195.6447 [M + 2H]$^{2+}$ (−2.33 ppm).

Synthesis of H4K16-Ac. To a solution of **H4K16-Ac-protected** (107 mg, 0.049 mmol) in CH_2Cl_2 (3 mL) was added TFA (3 mL). The reaction mixture was stirred for 3 h at R.T. and then evaporated. The residue was purified by reversed-phase HPLC to afford **H4K16-Ac·3TFA** (54 mg, 0.034 mmol) in 70% yield as a white solid. Purity by HPLC: 99.6% (254 nm); t_R = 6.66 min (A/B = 80:20 → 0:100 (20 min); A: 0.1% TFA Milli-Q, B: 0.1% TFA CH_3CN); HRMS (ESI$^+$): calcd: 1237.65809; found: 1237.65929 [M + 2H]$^{2+}$ (+0.97 ppm).

Synthesis of H4K16-Myr. To a solution of **H4K16-Myr-protected** (56 mg, 0.024 mmol) in CH_2Cl_2 (3 mL) was added TFA (3 mL). The reaction mixture was stirred for 3 h at R.T. and then evaporated. The residue was purified by reversed-phase HPLC to afford **H4K16-Myr·3TFA** (27 mg, 0.016 mmol) in 65% yield as a white solid. Purity by HPLC: 99.3% (254 nm); t_R = 11.9 min (A/B = 80:20 → 0:100 (20 min); A: 0.1% TFA Milli-Q, B: 0.1% TFA CH_3CN); HRMS (ESI$^+$): calcd: 1405.8459; found: 1405.8494 [M + 2H]$^{2+}$ (+2.51 ppm).

In Vitro Assay. *Absorption Measurement.* Absorption spectra were measured in a quartz cuvette (4 × 4 × 40 mm^3) on a UV-1800 instrument (Shimadzu, Japan). Spectra of **RIK^{Tfa}RY** and **S2DMi-1−14** were measured in Dulbecco's phosphate-buffered saline (Sigma), and the final concentration of each was 5 μm (0.2% DMSO).

Evaluation of SIRT2-Inhibitory Activity by the SFP3 Assay. **RIK^{Tfa}RY**, **S2DMi-1−14**, compound **6**, compound **M**, compound **TM**, AGK2, NAM, and SirReal2 were each dissolved in DMSO or Milli-Q (for NAM) and diluted as required with SIRT assay buffer I (Tris−HCl (pH 8.0), containing 150 mM NaCl, 1 mM DTT, and 0.05% Triton X-100) (×4 conc. 0.8% DMSO or 2% DMSO (for AGK2 and NAM)). SIRT2 (final 35 nM, 10 μL) was finally added to a solution of 2.5 μM SFP3 (10 μL), 500 μM NAD$^+$ (10 μL), and the indicated concentrations of SIRT2 inhibitor (10 μL, final 0.2% DMSO or 0.5% DMSO (for AGK2 and NAM)) in SIRT assay buffer I. Fluorescence intensity was measured at 5 min intervals with an ARVO X5 plate reader (filters: Ex = 485/14 nm, Em = 535/25 nm) for 60 min at 37 °C. IC_{50} values were calculated by using GraphPad Prism6. The results are shown as mean ± S.D. (n = 3).

Evaluation of SIRT2-Inhibitory Activity by the p53(Myr)-AMC (deMyr Activity) Assay. **RIK^{Tfa}RY**, **S2DMi-1−14**, compound **6**, compound **M**, compound **TM**, AGK2, NAM, and SirReal2 were each dissolved in DMSO or Milli-Q (for NAM) and diluted as required with SIRT assay buffer I (×4 conc. 2% DMSO). SIRT2 (final 70 nM, 5 μL) was finally added to a solution of **p53(Myr)-AMC** (final 50 μM, 5 μL), NAD$^+$ (final 500 μM, 5 μL), and the indicated concentrations of SIRT2 inhibitor (final 0.5% DMSO, 5 μL) in SIRT assay buffer I. Plates were incubated at R.T. for 3 h, and then a solution (20 μL) of trypsin (final 100 nM) and nicotinamide (final 1 mM) in SIRT assay buffer I was added. Fluorescence intensity was measured at 5 min intervals with an ARVO X5 plate reader (filters: Ex = 355/40 nm, Em = 460/25 nm) for 20 min at 37 °C. IC_{50} values were calculated by using GraphPad Prism6. The results are shown as mean ± S.D. (n = 3).

Evaluation of SIRT2-Inhibitory Activity by the FLUOR DE LYS SIRT2 Kit Assay. **RIK^{Tfa}RY**, **S2DMi-1−14**, compound **6**, compound **M**, compound **TM**, AGK2, NAM, and SirReal2 were dissolved in DMSO or Milli-Q (for NAM) and diluted as required with sirtuin assay buffer II (50 mM Tris−HCl (pH 8.0), containing 137 mM NaCl, 2.7 mM KCl, 1 mM $MgCl_2$, 1 mg/mL bovine serum albumin (BSA)) (×4 conc. 2% DMSO). SIRT2 (final 2 U, 5 μL) was finally added to a solution of deacetylase substrate (final 50 μM; 5 μL), NAD$^+$ (final 500 μM; 5 μL), and the indicated concentrations of SIRT2 inhibitor (final 0.5% DMSO, 5 μL) in sirtuin assay buffer II. Plates were incubated at R.T. for 2 h; then, a solution (20 μL) of Developer II and nicotinamide (final 2 mM) was added to each well. Fluorescence intensity was measured at 5 min intervals with an ARVO X5 plate reader (filters: Ex = 355/40 nm, Em = 460/25 nm) for 30 min at 37 °C. IC_{50} values were calculated by using GraphPad Prism6. The results are shown as mean ± S.D. (n = 3).

Evaluation of Inhibitory Activity against Developer II by the FLUOR DE LYS SIRT2 Kit Assay. **RIK^{Tfa}RY**, **S2DMi-1−14**, compound **M**, compound **TM**, AGK2, NAM, and SirReal2 were dissolved in DMSO or Milli-Q (for NAM) and diluted as required with sirtuin assay buffer II (50 mM Tris−HCl (pH 8.0), containing 137 mM NaCl, 2.7 mM KCl, 1 mM $MgCl_2$, 1 mg/mL BSA) (×4 conc. 2% DMSO). 1/200 diluted Developer II (final 1/400 dilution; 20 μL) was finally added to a solution of deacetylated standard substrate (final 50 μM; 10 μL) and SIRT2 inhibitor (final 1 μM, 0.5% DMSO, 10 μL) in sirtuin assay buffer II. Fluorescence intensity was measured at 5 min intervals with an ARVO X5 plate reader (filters: Ex = 355/40 nm, Em = 460/25 nm) for 20 min at 37 °C. The results are shown as mean ± S.D. (n = 3).

Evaluation of SIRT1-Inhibitory Activity by the SFP3 Assay. **RIK^{Tfa}RY**, **S2DMi-1−14**, compound **6**, compound **M**, compound **TM**, AGK2, NAM, and SirReal2 were dissolved in DMSO or Milli-Q (for NAM) and diluted as required with SIRT assay buffer I (Tris−HCl (pH 8.0), containing 150 mM NaCl, 1 mM DTT, 0.05% Triton

DOI: 10.1021/acs.jmedchem.9b00315
J. Med. Chem. XXXX, XXX, XXX−XXX

X-100) (×4 conc. 0.8% DMSO or 2% DMSO (for AGK2 and nicotinamide)). SIRT1 (final 7 nM, 10 μL) was finally added to a solution of 2.5 μM SFP3 (10 μL), 500 μM NAD^+ (10 μL), and the indicated concentrations of SIRT2 inhibitor (10 μL, final 0.2% DMSO or 0.5% DMSO (for AGK2 and nicotinamide)) in SIRT assay buffer I. Fluorescence intensity was measured at 5 min intervals with an ARVO X5 plate reader (filters: Ex = 485/14 nm, Em = 535/25 nm) for 60 min at 37 °C. IC_{50} values were calculated by using GraphPad Prism6. The results are shown as mean ± S.D. (n = 3).

Evaluation of SIRT1-Inhibitory Activity by the p53(Myr)-AMC Assay (deMyr Activity). **RIK^{Tfa}RY**, **S2DMi-1−14**, compound **6**, compound **M**, compound **TM**, AGK2, and SirReal2 were dissolved in DMSO and diluted as required with SIRT assay buffer I (×4 conc. 2% DMSO). SIRT1 (final 14 nM, 5 μL) was finally added to a solution of **p53(Myr)-AMC** (final 50 μM, 5 μL), NAD^+ (final 500 μM, 5 μL), and the indicated concentrations of SIRT2 inhibitor (final 0.5% DMSO, 5 μL) in SIRT assay buffer I. Plates were incubated at R.T. for 3 h, and then a solution (20 μL) of trypsin (final 100 nM) and nicotinamide (final 1 mM) in SIRT assay buffer I was added. Fluorescence intensity was measured at 5 min intervals with an ARVO X5 plate reader (filters: Ex = 355/40 nm, Em = 460/25 nm) for 20 min at 37 °C. IC_{50} values were calculated by using GraphPad Prism6. The results are shown as mean ± S.D. (n = 3).

Evaluation of SIRT3-Inhibitory Activity by the SFP3 Assay. **RIK^{Tfa}RY**, **S2DMi-1−12**, compound **M**, compound **TM**, AGK2, and NAM were dissolved in DMSO or Milli-Q (for NAM) and diluted as required with SIRT assay buffer I (Tris−HCl (pH 8.0), containing 150 mM NaCl, 1 mM DTT, 0.05% Triton X-100) (×4 conc. 0.8% DMSO or 2% DMSO (for AGK2 and NAM)). SIRT3 (final 60 nM, 10 μL) was finally added to a solution of 2.5 μM SFP3 (10 μL), 500 μM NAD^+ (10 μL), and the indicated concentrations of SIRT2 inhibitor (10 μL, final 0.2% DMSO or 0.5% DMSO (for AGK2 and NAM)) in SIRT assay buffer I. Fluorescence intensity was measured at 5 min intervals with an ARVO X5 plate reader (filters: Ex = 485/14 nm, Em = 535/25 nm) for 60 min at 37 °C. IC_{50} values were calculated by using GraphPad Prism6. The results are shown as mean ± S.D. (n = 3).

Evaluation of SIRT3-Inhibitory Activity by the p53(Myr)-AMC Assay (deMyr Activity). **RIK^{Tfa}RY**, **S2DMi-1−12**, compound **M**, compound **TM**, and AGK2 were dissolved in DMSO and diluted as required with SIRT assay buffer I (×4 conc. 2% DMSO). SIRT3 (final 120 nM, 5 μL) was finally added to a solution of **p53(Myr)-AMC** (final 50 μM, 5 μL), NAD^+ (final 500 μM, 5 μL), and the indicated concentrations of SIRT2 inhibitor (final 0.5% DMSO, 5 μL) in SIRT assay buffer I. Plates were incubated at R.T. for 3 h, and then a solution (20 μL) of trypsin (final 100 nM) and nicotinamide (final 1 mM) in SIRT assay buffer I was added. Fluorescence intensity was measured at 5 min intervals with an ARVO X5 plate reader (filters: Ex = 355/40 nm, Em = 460/25 nm) for 20 min at 37 °C. IC_{50} values were calculated by using GraphPad Prism6. The results are shown as mean ± S.D. (n = 3).

Evaluation of SIRT6-Inhibitory Activity by the SFP3 Assay. **RIK^{Tfa}RY**, **S2DMi-1−14**, compound **M**, compound **TM**, and SirReal2 were dissolved in DMSO and diluted as required with SIRT assay buffer I (Tris−HCl (pH 8.0), containing 150 mM NaCl, 1 mM DTT, 0.05% Triton X-100) (×4 conc. 0.8% DMSO). SIRT6 (final 48 nM, 10 μL) was finally added to the solution of 2.5 μM SFP3 (10 μL), 500 μM NAD^+ (10 μL), and the indicated concentrations of SIRT2 inhibitor (10 μL, final 0.2% DMSO) in SIRT assay buffer I. Fluorescence intensity was measured at 5 min intervals with an ARVO X5 plate reader (filters: Ex = 485/14 nm, Em = 535/25 nm) for 60 min at 37 °C. IC_{50} values were calculated by using GraphPad Prism6. The results are shown as mean ± S.D. (n = 3).

HPLC Analysis of SIRT2-Mediated Cleavage of p53(Myr)-AMC. **p53(Myr)-AMC** (final 50 μM, 0.5% DMSO) was incubated in SIRT assay buffer I, containing 500 μM NAD^+ and 175 nM SIRT2 at 37 °C. Aliquots (20 μL) were taken at 0 and 1 h and analyzed by HPLC. HPLC conditions: A/B = 99:1 (initial) → 0:100 (20 min) → 0:100 (23 min) with a linear gradient, A = 0.1% FA Milli-Q, B = 0.1% FA CH_3CN. Absorbance was monitored at 325 nm.

HPLC Analysis of the Stability of SIRT2 Inhibitors in the Presence of SIRT2. **S2DMi-1−3**, **S2DMi-6**, and **S2DMi-9** were each dissolved in DMSO (10 mM) and diluted as required with SIRT assay buffer I (200 μM, 2% DMSO). SIRT2 (final 350 nM) was added to the solutions of SIRT2 inhibitors (final 20 μM, 0.2% DMSO) and NAD^+ (final 500 μM) in SIRT assay buffer I. Each mixture was incubated at 37 °C. Aliquots (20 μL) were taken at 0 and 4 h and analyzed by HPLC. HPLC conditions: A/B = 80:20 (initial) → 0:100 (20 min) → 0:100 (23 min) with a linear gradient, A = 0.1% TFA Milli-Q, B = 0.1% TFA CH_3CN. Absorbance was monitored at 510 nm (**S2DMi-1−3**), 350 nm (**S2DMi-6**), or 254 nm (**S2DMi-9**).

Competition Assay with SFP3 (Lineweaver−Burk Plots and Michaelis−Menten Plots). SIRT2 (final 35 nM, 10 μL) was added to a solution of SFP3 (final 0.625, 1.25, and 2.5 μM, 10 μL) and 500 μM NAD^+ and **S2DMi-6** or **S2DMi-9** (final 15, 20, and 30 nM, 0.2% DMSO, 10 μL) in SIRT assay buffer I. Fluorescence intensity was measured at 1 min intervals with an ARVO X5 plate reader (filters: Ex = 485/14 nm, Em = 535/25 nm) for 30 min at 37 °C. The K_m and V_{max} values were calculated by using GraphPad Prism6. The rate of fluorescence increase (v; fluorescence intensity/min) over 20 min (from 10 to 30 min) was calculated, and a double-reciprocal plot of initial velocity as a function of substrate concentration, $1/v$ against 1/[SFP3], was drawn. The results are shown as mean ± S.D. (n = 3)

Competition Assay with NAD^+ (Lineweaver−Burk Plots and Michaelis−Menten Plots). SIRT2 (final 35 nM, 10 μL) was added to a solution of SFP3 (final 2.5 μM, 10 μL) and NAD^+ (6.7, 20, and 60 μM) and **S2DMi-6** or **S2DMi-9** (final 15, 20, and 30 nM, 0.2% DMSO, 10 μL) in SIRT assay buffer I. Fluorescence intensity was measured at 1 min intervals with an ARVO X5 plate reader (filters: Ex = 485/14 nm, Em = 535/25 nm) for 30 min at 37 °C. The K_m and V_{max} values were calculated by using GraphPad Prism6. The rate of fluorescence increase (v; fluorescence intensity/min) over 10 min (from 10 to 30 min) was calculated, and a double-reciprocal plot of initial velocity as a function of substrate concentration, $1/v$ against 1/[SFP3], was drawn. The results are shown as mean ± S.D. (n = 3)

HPLC Analysis of SIRT2-Mediated Demyristoylation of H4K16-Myr and Inhibition Assay. **H4K16-Myr** (final 100 μM, 0.5% DMSO) was incubated in SIRT assay buffer I without 1 mM DTT, containing 500 μM NAD^+ and 175 nM SIRT2 at 37 °C for 2 h in the presence or absence of SIRT2 inhibitors (**S2DMi-6**, **S2DMi-7**, **S2DMi-9** (0.1, 1, 10 μM, 0.5% DMSO), compound **TM** (10 μM, 0.5% DMSO), AGK2 (50 μM, 0.5% DMSO), SirReal2 (10 μM, 0.5% DMSO), NAM (500 μM, 0.5% DMSO)). The reactions were stopped using 20 μL of 1 N HCl in MeOH. Aliquots (20 μL) were taken and analyzed by HPLC. HPLC conditions: A/B = 80:20 (initial) → 0:100 (20 min) → 0:100 (25 min) with a linear gradient, A = 0.1% TFA Milli-Q, B = 0.1% TFA CH_3CN. Absorbance was monitored at 280 nm.

HPLC Analysis of SIRT2-Mediated Deacetylation of H4K16-Ac and Inhibition Assay. **H4K16-Ac** (final 100 μM, 0.5% DMSO) was incubated in SIRT assay buffer I without 1 mM DTT, containing 500 μM NAD^+ and 175 nM SIRT2 at 37 °C for 30 min in the presence or absence of SIRT2 inhibitors (**S2DMi-6**, **S2DMi-7**, **S2DMi-9** (0.01, 0.1, 1, 10 μM, 0.5% DMSO), and NAM (500 μM, 0.5% DMSO)). The reactions were stopped using 20 μL of 1 N HCl in MeOH. Aliquots (20 μL) were taken and analyzed by HPLC. HPLC conditions: A/B = 80:20 (initial) → 0:100 (20 min) → 0:100 (25 min) with a linear gradient, A = 0.1% TFA Milli-Q, B = 0.1% TFA CH_3CN. Absorbance was monitored at 280 nm.

Determination of Kinetic Parameters of H4K16-Ac and H4K16-Myr toward SIRT2. For kinetics analysis, 70 nM (for **H4K16-Ac**) or 10 nM (for **H4K16-Myr**) SIRT2 was incubated in 20 μL of SIRT assay buffer I without 1 mM DTT, containing 500 μM NAD^+ with **H4K16-Ac** or **H4K16-Myr** at varied concentrations at 37 °C for 600 s (for **H4K16-Ac**) or 320 s (for **H4K16-Myr**). Peptide concentrations used for **H4K16-Ac** were 1, 2, 4, 8, 16, 32, and 64 μM and those for **H4K16-Myr** were 0.25, 0.5, 1, 2, 4, 8, and 16 μM. The reactions were stopped using 10 μL of 2 N HCl in MeOH. Aliquots (20 μL) were taken and analyzed by HPLC. HPLC conditions: A/B = 80:20 (initial) → 0:100 (20 min) → 0:100 (25 min) with a linear

DOI: 10.1021/acs.jmedchem.9b00315
J. Med. Chem. XXXX, XXX, XXX−XXX

gradient, A = 0.1% TFA Milli-Q, B = 0.1% TFA CH_3CN. The product and substrate peaks were quantified by integrating the area at 280 nm, which were converted to initial velocity (μM/s). The velocities were plotted against the peptide concentrations, and then K_m and V_{max} values were calculated by using GraphPad Prism6.

Cell Viability Assay Using CCK-8 Reagent. HeLa cells (1.0×10^4 cells) were grown on a PLL-coated 96-well microplate (IWAKI) overnight in 100 μL of Dulbecco's modified Eagle's medium (DMEM) (10% fetal bovine serum and penicillin (100 units/mL) and streptomycin (100 μg/mL)) in a humidified incubator containing 5% CO_2 in air at 37 °C for 24 h. Various concentrations (final 1.56, 3.13, 6.25, 6.25, 12.5, 25, 50 μM) of compounds (compound **TM**, **S2DMi-6**, **S2DMi-7** and **S2DMi-9**) or DMSO (control) in DMEM (2% DMSO, 10 μL) were added to each well and further incubated for 72 h. CCK-8 reagent (10 μL) was added to each well and incubated at 37 °C for 2 h, and then absorption at 450 nm was measured with an ARVO X5 plate reader.

■ ASSOCIATED CONTENT

Supporting Information

The Supporting Information is available free of charge on the ACS Publications website at DOI: 10.1021/acs.jmedchem.9b00315.

Absorbance spectra of synthesized compounds; SIRT inhibition curves of synthesized compounds and known SIRT2 inhibitors toward SIRT1−3, and 6 in SFP3, **p53(Myr)-AMC**, and FLUOR DE LYS SIRT2 kit assays; Michaelis−Menten plots of **H4K16-Ac** and **H4K16-Myr** against SIRT2; SIRT2 deacetylase inhibition assay using **H4K16-Ac** peptide; cell viability assay using HeLa cells; competition analysis of **S2DMi-6** and **S2DMi-9** with NAD^+; purity data of all synthesized compounds by HPLC and enantiomerical purity data of compounds **1−6** (PDF)

Molecular formula strings and enzyme inhibition data (CSV)

■ AUTHOR INFORMATION

Corresponding Author

*E-mail: deco@phar.nagoya-cu.ac.jp. Tel: +81-52-836-3407. Fax: +81-52-836-3407.

ORCID

Hidehiko Nakagawa: 0000-0001-8435-4401

Notes

The authors declare no competing financial interest.

■ ACKNOWLEDGMENTS

The authors thank Drs. Hiroyuki Yamakoshi and Seiichi Nakamura at Nagoya City University for help and advice for the chiral column HPLC experiment and thank all of the members of H.N.'s laboratory for fruitful discussions. This work was supported in part by JSPS KAKENHI Grant Numbers 26893223, 15K18899 (M.K.) and 16H05103 (H.N.), as well as by the Hori Sciences and Arts Foundation (M.K.), Mochida Memorial Foundation for Medical and Pharmaceutical Research (M.K.), a Grant-in-Aid for Scientific Research on Innovative Areas from MEXT (26111012, H.N.), and a grant from Daiichi Sankyo Foundation of Life Science (H.N.).

■ ABBREVIATIONS

SIRT, sirtuin; NAD, nicotinamide adenine dinucleotide; TNF-α, tumor necrosis factor α; AMC, 7-amino-4-methylcoumarin; Dabcyl, 4-(4-(dimethylamino)phenylazo)benzoic acid; NAM, nicotinamide; DTT, dithiothreitol

■ REFERENCES

(1) Imai, S.; Armstrong, C. M.; Kaeberlein, M.; Guarente, L. Transcriptional Silencing and Longevity Protein Sir2 is an NAD-Dependent Histone Deacetylase. *Nature* **2000**, *403*, 795−800.

(2) Houtkooper, R. H.; Pirinen, E.; Auwerx, J. Sirtuins as Regulators of Metabolism and Healthspan. *Nat. Rev. Mol. Cell Biol.* **2012**, *13*, 225−238.

(3) Haigis, M. C.; Guarente, L. P. Mammalian Sirtuins-Emerging Roles in Physiology, Aging, and Calorie Restriction. *Genes Dev.* **2006**, *20*, 2913−2921.

(4) Longo, V. D.; Kennedy, B. K. Sirtuins in Aging and Age-Related Disease. *Cell* **2006**, *126*, 257−268.

(5) Sauve, A. A.; Wolberger, C.; Schramm, V. L.; Boeke, J. D. The Biochemistry of Sirtuins. *Annu. Rev. Biochem.* **2006**, *75*, 435−465.

(6) Finkel, T.; Deng, C. X.; Mostoslavsky, R. Recent Progress in the Biology and Physiology of Sirtuins. *Nature* **2009**, *460*, 587−591.

(7) Mathias, R. A.; Greco, T. M.; Oberstein, A.; Budayeva, H. G.; Chakrabarti, R.; Rowland, E. A.; Kang, Y.; Shenk, T.; Cristea, I. M. Sirtuin 4 is a Lipoamidase Regulating Pyruvate Dehydrogenase Complex Activity. *Cell* **2014**, *159*, 1615−1625.

(8) Du, J.; Zhou, Y.; Su, X.; Yu, J. J.; Khan, S.; Jiang, H.; Kim, J.; Woo, J.; Kim, J. H.; Choi, B. H.; He, B.; Chen, W.; Zhang, S.; Cerione, R. A.; Auwerx, J.; Hao, Q.; Lin, H. Sirt5 is a NAD-Dependent Protein Lysine Demalonylase and Desuccinylase. *Science* **2011**, *334*, 806−809.

(9) Jiang, H.; Khan, S.; Wang, Y.; Charron, G.; He, B.; Sebastian, C.; Du, J.; Kim, R.; Ge, E.; Mostoslavsky, R.; Hang, H. C.; Hao, Q.; Lin, H. SIRT6 Regulates TNF-α Secretion Through Hydrolysis of Long-Chain Fatty Acyl Lysine. *Nature* **2013**, *496*, 110−113.

(10) Li, L.; Shi, L.; Yang, S.; Yan, R.; Zhang, D.; Yang, J.; He, L.; Li, W.; Yi, X.; Sun, L.; Liang, J.; Cheng, Z.; Shi, L.; Shang, Y. SIRT7 is a Histone Desuccinylase that Functionally Links to Chromatin Compaction and Genome Stability. *Nat. Commun.* **2016**, *7*, No. 12235.

(11) Feldman, J. L.; Baeza, J.; Denu, J. M. Activation of the Protein Deacetylase SIRT6 by Long-Chain Fatty Acids and Widespread Deacylation by Mammalian Sirtuins. *J. Biol. Chem.* **2013**, *288*, 31350−31356.

(12) Teng, Y. B.; Jing, H.; Aramsangtienchai, P.; He, B.; Khan, S.; Hu, J.; Lin, H.; Hao, Q. Efficient Demyristoylase Activity of SIRT2 Revealed by Kinetic and Structural Studies. *Sci. Rep.* **2015**, *5*, No. 8529.

(13) Wang, Y.; Fung, Y. M. E.; Zhang, W.; He, B.; Chung, M. W. H.; Jin, J.; Hu, J.; Lin, H.; Hao, Q. Deacylation Mechanism by SIRT2 Revealed in the 1′-SH-2′-O-Myristoyl Intermediate Structure. *Cell Chem. Biol.* **2017**, *24*, 339−345.

(14) Lanyon-Hogg, T.; Faronato, M.; Serwa, R. A.; Tate, E. W. Dynamic Protein Acylation: New Substrates, Mechanisms, and Drug Targets. *Trends Biochem. Sci.* **2017**, *42*, 566−581.

(15) Tate, E. W.; Kalesh, K. A.; Lanyon-Hogg, T.; Storck, E. M.; Thinon, E. Global Profiling of Protein Lipidation Using Chemical Proteomic Technologies. *Curr. Opin. Chem. Biol.* **2015**, *24*, 48−57.

(16) Jing, H.; Zhang, X.; Wisner, S. A.; Chen, X.; Spiegelman, N. A.; Linder, M. E.; Lin, H. SIRT2 and Lysine Fatty Acylation Regulate the Transforming Activity of K-Ras4a. *eLife* **2017**, *6*, No. e32436.

(17) Zhang, X.; Khan, S.; Jiang, H.; Antonyak, M. A.; Chen, X.; Spiegelman, N. A.; Shrimp, J. H.; Cerione, R. A.; Lin, H. Identifying the Functional Contribution of the Defatty-Acylase Activity of SIRT6. *Nat. Chem. Biol.* **2016**, *12*, 614−620.

(18) Rotili, D.; Tarantino, D.; Nebbioso, A.; Paolini, C.; Huidobro, C.; Lara, E.; Mellini, P.; Lenoci, A.; Pezzi, R.; Botta, G.; Lahtela-Kakkonen, M.; Poso, A.; Steinkühler, C.; Gallinari, P.; De Maria, R.; Fraga, M.; Esteller, M.; Altucci, L.; Mai, A. Discovery of Salermide-Related Sirtuin Inhibitors: Binding Mode Studies and Antiproliferative Effects in Cancer Cells Including Cancer Stem Cells. *J. Med. Chem.* **2012**, *55*, 10937−10947.

DOI: 10.1021/acs.jmedchem.9b00315
J. Med. Chem. XXXX, XXX, XXX−XXX

(19) Jing, H.; Hu, J.; He, B.; Negrón Abril, Y. L.; Stupinski, J.; Weiser, K.; Carbonaro, M.; Chiang, Y. L.; Southard, T.; Giannakakou, P.; Weiss, R. S.; Lin, H. A SIRT2-Selective Inhibitor Promotes c-Myc Oncoprotein Degradation and Exhibits Broad Anticancer Activity. *Cancer Cell* **2016**, *29*, 297−310.

(20) Rumpf, T.; Schiedel, M.; Karaman, B.; Roessler, C.; North, B. J.; Lehotzky, A.; Oláh, J.; Ladwein, K. I.; Schmidtkunz, K.; Gajer, M.; Pannek, M.; Steegborn, C.; Sinclair, D. A.; Gerhardt, S.; Ovádi, J.; Schutkowski, M.; Sippl, W.; Einsle, O.; Jung, M. Selective Sirt2 Inhibition by Ligand-Induced Rearrangement of the Active Site. *Nat. Commun* **2015**, *6*, No. 6263.

(21) Outeiro, T. F.; Kontopoulos, E.; Altmann, S. M.; Kufareval, I.; Strathearn, K. E.; Amore, A. M.; Volk, C. B.; Maxwell, M. M.; Rochet, J. C.; McLean, P. J.; Young, A. B.; Abagyan, R.; Feany, M. B.; Hyman, B. T.; Kazantsev, A. G. Sirtuin 2 Inhibitors Rescue Alpha-Synuclein-Mediated Toxicity in Models of Parkinson's Disease. *Science* **2007**, *317*, 516−519.

(22) Mellini, P.; Itoh, Y.; Tsumoto, H.; Li, Y.; Suzuki, M.; Tokuda, N.; Kakizawa, T.; Miura, Y.; Takeuchi, J.; Lahtela-Kakkonen, M.; Suzuki, T. Potent Mechanism-Based Sirtuin-2-Selective Inhibition by an *in situ*-Generated Occupant of the Substrate-Binding Site, "Selectivity Pocket" and NAD^+-Binding Site. *Chem. Sci.* **2017**, *8*, 6400−6408.

(23) Kudo, N.; Ito, A.; Arata, M.; Nakata, A.; Yoshida, M. Identification of a Novel Small Molecule that Inhibits Deacetylase but not Defatty-Acylase Reaction Catalysed by SIRT2. *Philos. Trans. R. Soc., B* **2018**, *373*, No. 20170070.

(24) Swyter, S.; Schiedel, M.; Monaldi, D.; Szunyogh, S.; Lehotzky, A.; Rumpf, T.; Ovádi, J.; Sippl, W.; Jung, M. New Chemical Tools for Probing Activity and Inhibition of the NAD^+-Dependent Lysine Deacylase Sirtuin 2. *Philos. Trans. R. Soc., B* **2018**, *373*, No. 20170083.

(25) Spiegelman, N. A.; Price, I. R.; Jing, H.; Wang, M.; Yang, M.; Cao, J.; Hong, J. Y.; Zhang, X.; Aramsangtienchai, P.; Sadhukhan, S.; Lin, H. Direct Comparison of SIRT2 Inhibitors: Potency, Specificity, Activity-Dependent Inhibition, and On-Target Anticancer Activities. *ChemMedChem* **2018**, *13*, 1890−1894.

(26) Spiegelman, N. A.; Hong, J. Y.; Hu, J.; Jing, H.; Wang, M.; Price, I. R.; Cao, J.; Yang, M.; Zhang, X.; Lin, H. A Small-Molecule SIRT2 Inhibitor that Promotes K-Ras4a Lysine Fatty-Acylation. *ChemMedChem* **2019**, 744−748.

(27) Yang, L. L.; Xu, W.; Yan, J.; Su, H. L.; Yuan, C.; Li, C.; Zhang, X.; Yu, Z. J.; Yan, Y. H.; Yu, Y.; Chen, Q.; Wang, Z.; Li, L.; Qian, S.; Li, G. B. Crystallographic and SAR Analyses Reveal the High Requirements Needed to Selectively and Potently Inhibit SIRT2 Deacetylase and Decanoylase. *MedChemComm* **2019**, *10*, 164−168.

(28) Morimoto, J.; Hayashi, Y.; Suga, H. Discovery of Macrocyclic Peptides Armed with a Mechanism-Based Warhead: Isoform-Selective Inhibition of Human Deacetylase SIRT2. *Angew. Chem., Int. Ed.* **2012**, *51*, 3423−3427.

(29) Kawaguchi, M.; Ikegawa, S.; Ieda, N.; Nakagawa, H. A Fluorescent Probe for Imaging Sirtuin Activity in Living Cells, Based on One-Step Cleavage of the Dabcyl Quencher. *ChemBioChem* **2016**, *17*, 1961−1967.

(30) Huang, H.; Zhang, D.; Wang, Y.; Perez-Neut, M.; Han, Z.; Zheng, Y. G.; Hao, Q.; Zhao, Y. Lysine Benzoylation is a Histone Mark Regulated by SIRT2. *Nat. Commun.* **2018**, *9*, No. 3374.

(31) Zhang, X.; Spiegelman, N. A.; Nelson, O. D.; Jing, H.; Lin, H. SIRT6 Regulates Ras-Related Protein R-Ras2 by Lysine Defatty-Acylation. *eLife* **2017**, *6*, No. e25158.

DOI: 10.1021/acs.jmedchem.9b00315
J. Med. Chem. XXXX, XXX, XXX−XXX